OCEAN ENGINEERING GROUP

TIP FLOWS FOR WINGS AND PROPELLERS AND THEIR EFFECT ON THE PREDICTED PERFORMANCE

S.A. Kinnas and S. Pyo

Report No. 98-1

ENVIRONMENTAL AND WATER RESOURCES ENGINEERING
DEPARTMENT OF CIVIL ENGINEERING
THE UNIVERSITY OF TEXAS AT AUSTIN
Austin, TX 78712

REPORT DOCUMENTATION PAGE

Form Approved
OMB No. 0704-0188

1. AGENCY USE ONLY (Leave blank)	2. REPORT DATE	3. REPORT TYPE AND DATES COVERED
	January 1998	Final Report

4. TITLE AND SUBTITLE
Tip flows for wings and propellers and their effect on the predicted performance

5. FUNDING NUMBERS
N00014-96-1-0231

6. AUTHOR(S)
Spyros A. Kinnas & Sangwoo Pyo

7. PERFORMING ORGANIZATION NAME(S) AND ADDRESS(ES)
Ocean Engineering Group
Department of Civil Engineeering
The University of Texas at Austin
Austin, TX 78712

8. PERFORMING ORGANIZATION REPORT NUMBER
98-1

9. SPONSORING/MONITORING AGENCY NAME(S) AND ADDRESS(ES)
Office of Naval Research
800 North Quincy St.
Arlington, VA 22217-5600

10. SPONSORING/MONITORING AGENCY REPORT NUMBER

11. SUPPLEMENTARY NOTES

12a. DISTRIBUTION/AVAILABILITY STATEMENT
Approved for public release; distribution unlimited

12b. DISTRIBUTION CODE

13. ABSTRACT *(Maximum 200 words)*

Various wake alignment techniques which have been developed in the past for the analysis of noncavitating propellers in uniform inflows are reviewed and some of them are extended in the case of caviatting flows subject to inclined inflows. The effect of the inclined trailing wake geometry on the predicted cavities and blade forces is found to be significant. The effect of the tip vortex detachment location on the shape of the trailing wake and on the pressure distribution on the tip is studied for wings and propeller blades. The local viscous flow inside of the core of a tip vortex is formulated via a parabolic Navier-Stokes approach. Predicted open flow characteristics and unsteady forces acting on the blades of an inclined shaft propeller are compared to those predicted by other methods, as well as those measured in experiments.

14. SUBJECT TERMS
Tip vortex, Cavitation, Propeller performance, Wake alignment, Inclined flows

15. NUMBER OF PAGES
42

16. PRICE CODE

17. SECURITY CLASSIFICATION OF REPORT	18. SECURITY CLASSIFICATION OF THIS PAGE	19. SECURITY CLASSIFICATION OF ABSTRACT	20. LIMITATION OF ABSTRACT
Unclassified	Unclassified	Unclassified	

TIP FLOWS FOR WINGS AND PROPELLERS AND THEIR EFFECT ON THE PREDICTED PERFORMANCE

by S.A. Kinnas and S. Pyo
Department of Civil Engineering
The University of Texas at Austin

Ocean Engineering Report 98-1

January 1998

The preparation of this document was carried out under the
Office of Naval Research
ONR Contract No. N00014-96-1-0231
UT-OSP 26-06750-55

TIP FLOWS FOR WINGS AND PROPELLERS AND THEIR EFFECT ON THE PREDICTED PERFORMANCE

Spyros A. Kinnas[1] and Sangwoo Pyo[2]

ABSTRACT

Various wake alignment techniques which have been developed in the past for the analysis of non-cavitating propellers in uniform inflows are reviewed and some of them are extended in the case of cavitating flows subject to inclined inflows. The effect of the inclined trailing wake geometry on the predicted cavities and blade forces is found to be significant. The effect of the tip vortex detachment location on the shape of the trailing wake and on the pressure distribution on the tip is studied for wings and propeller blades. The local viscous flow inside of the core of a tip vortex is formulated via a parabolic Navier-Stokes approach. Predicted open flow characteristics and unsteady forces acting on the blades of an inclined shaft propeller are compared to those predicted by other methods, as well as those measured in experiments.

NOMENCLATURE

V_{IN} ; inflow velocity at the propeller plane

C_p ; pressure coefficient : $= (p - p_\infty)/(1/2)\rho V_S^2$

[1] Assistant Professor, Ocean Engineering Group, Department of Civil Engineering, The University of Texas at Austin, *kinnas@mail.utexas.edu*

[2] Postdoctoral associate, Ocean Engineering Group, Department of Civil Engineering, The University of Texas at Austin.

D ; propeller diameter

F_n ; Froude number based on propeller RPM; $= n^2D/g$

J_S ; advance coefficient based on ship speed : $= V_S/nD$

K_T ; trust coefficient : $= T/\rho n^2 D^4$

K_Q ; torque coefficient : $= Q/\rho n^2 D^5$

n ; propeller RPM

p ; pressure

p_v ; vapor pressure

p_∞ ; pressure at infinity (at the shaft depth)

V_S ; ship speed

θ ;angular coordinate of point on trailing wake surface

θ_B ;blade angle

σ_n ; cavitation number based on propeller RPM ; $= (p_\infty - p_v)/(1/2)\rho n^2 D^2$

ω ; propeller angular velocity

Acronyms - Names of computer codes

FLAG ; **FL**ow **A**dapted **G**rid

BEM ; **B**oundary **E**lement **M**ethod

VLM ; **V**ortex **L**attice **M**ethod

PSF-2 ; **P**ropeller blade analysis code in **S**teady **F**low based on VLM

PSF-2IS ; PSF-2, 1979 version includes **I**nclined **S**haft effects

PUF-2 ; **P**ropeller blade analysis code in **U**nsteady **F**low based on VLM

PUF-3 ; **P**ropeller **U** nsteady cavitating **F**low analysis code based on VLM, 1979 original version

PUF-3A ; PUF-3, 1986-93 versions includes leading edge correction

HPUF-3A ; PUF-3, 1994 version includes effects of **H**ub

HPUF-3AL/INC; PUF-3, 1996 version includes effects of wake **AL**ignment and effects of **INC**lined flow

PSF-10/PUF-10 ; Propeller blade analysis code in **S**teady/ **U**nsteady **F**low based on BEM

1 INTRODUCTION

The hydrodynamic analysis of lifting surfaces (wings or propeller blades) via potential flow methods requires knowledge of the shape of the trailing wake vorticity sheet. The location of the vortex sheet can be determined from the condition of zero pressure jump across the sheet, also known as the *force-free* wake condition. This condition is equivalent to requiring the potential jump in the wake to be convected with the resulting flow. The prediction of the evolution of a wake sheet has been studied extensively in the past and a review of the related bibliography with emphasis on marine propellers may be found in (Pyo 1995) and (Pyo & Kinnas 1997).

The effect of the main parameters of the wake geometry, such as pitch, transition wake length, and ultimate wake radius, on the predicted propeller thrust and torque was first studied in (Kerwin & Lee 1978). This wake model was also applied when the effects of unsteady sheet cavitation were included (Lee 1979). The importance of the wake geometry on the blade forces was also studied by (Hoshino 1991) who determined the wake shape experimentally by using an LDV system. The effect of the wake location becomes more crucial in the case of low advance ratios, as for example in the case of helicopter blades (Morino & Bharadvaj 1988), due to the effect of each blade's wake on the other blades. The effect of the wake location and detailed structure is also important in the case of a stage of a multi-component propulsor working in the wake of another.

In (Greeley & Kerwin 1982) an iterative procedure was developed to determine the wake geometry of a propeller in axisymmetric inflow. Later in (Keenan 1989) a method was developed for the treatment of the trailing wake in the case of non-axisymmetric inflows. These inflows are mainly due to the ship's viscous wake at the stern. However, the propeller blades will also be subject to unsteady flows in the case of inclined inflows. This inclination may be either due to an inclined shaft or due to a transverse inflow during maneuvering of the ocean vehicle. The blades will be subject to once per revolution sinusoidally varying inflow and thus unsteady forces, which may lead to fatigue and eventually deformation or damage of the blade (Boswell et al 1984). The effect of the inclined wake geometry on the prediction of the unsteady blade forces in the case of inclined inflow was studied in (Kerwin 1979) and found to be very critical. The effect of the inclined wake was evaluated at 0, 90, 180, and 270 degrees and interpolated in between.

In the present paper first a review of the existing wake models for marine propeller applications is given. The model of (Greeley & Kerwin 1982) is then extended in the case of cavitating flow. Finally an inclined wake model is developed in which the trailing wake is aligned (at each blade angle) with the axisymmetric flow to which the transverse flow due to the shaft inclination is superimposed. The predicted forces are compared to those measured in existing experiments.

2 UNIFORM INFLOW

2.1 Partial wake alignment

This model was developed first for the prediction of the propeller performance in steady or unsteady flows by using a VLM approach (Kerwin & Lee 1978). The corresponding code is called PUF-2. The trailing wake is divided into a transition and an ultimate wake region. In the transition region the trailing vorticity lines are assumed to converge to either the tip or the hub roll-up points depending on the sign of the vorticity strength[1]. The roll-up points are also the starting points for the concentrated tip or hub vortices in the ultimate wake region. The pitch angle, β_T, at the outer extremity of the transition region is taken by the following relationship:

$$\beta_T = \frac{\beta_{tip} + \phi_{0.7}}{2} \tag{1}$$

where β_{tip} is the hydrodynamic pitch angle of the undisturbed inflow and $\phi_{0.7}$ is the geometric pitch angle at $r = 0.7R$.

The pitch angle, β_W, of the concentrated tip vortex in the ultimate wake region is taken from the following relationship:

$$\beta_W = 1.15\beta_T \tag{2}$$

The extent of the transition wake is determined by the blade angle between the tip of the blade and the beginning of the ultimate wake. It is usually taken equal to 90^o. The radius of the ultimate wake is user specified and taken equal to 0.83 of the propeller radius[2].

This wake model was also applied in the case of cavitating flow (Lee 1979). The corresponding code is called PUF-3. It was found that this wake model was resulting to cavity sources in the trailing wake (in the case of super-cavitating flows) the total value of which was inconsistent with the value of the cavity volume velocity (Kinnas 1983). This inconsistency was resolved by not allowing for either roll-up or contraction of the trailing wake lines (Kinnas 1983). The revised code is called PUF-3A[3]. The corresponding wake model is shown in Figure 1. Note that the transition region has been doubled (from a blade angle of 90^o to 180^o) to accommodate longer super-cavities in one of the most recent versions, HPUF-3AL (Pyo & Kinnas 1996).

[1] This technique is accounting for the increase in the strength of the tip vortex in a semi-empirical manner without actually treating the mechanism of the "wake roll-up"

[2] This value was measured over a wide range of propeller geometries and advance ratios (Kerwin & Lee 1978).

[3] This version also included the leading edge correction (Kinnas 1991, Kerwin et al 1986).

2.2 Wake alignment without roll-up

Equation (1) provides partial dependency of the trailing wake on the incoming flow. An iterative procedure that aligns the trailing wake geometry with the resulting flow was developed in (Greeley & Kerwin 1982). The corresponding code is called PSF-2. The wake is again divided into the transition and the ultimate region. The trailing vortex lines are aligned with the actual (computed) flow at the start (blade trailing edge) and at the end of the transition wake region, while interpolated in between. Only the axial and tangential velocities induced by the propeller are being used in this procedure. The radial location of the vortex lines is determined in terms of the contraction of the transition wake at the tip and the ultimate wake radius, both of which are inputs taken from experimental observations. In this way the wake roll-up is suppressed. The ultimate wake pitch is determined by using the method developed in (Loukakis 1971) where the ultimate wake is assumed to extent infinitely upstream and downstream. This wake model is depicted in Figure 2.

This method was also applied in the case of the representation of the blade with a boundary element (panel) method for steady (Lee 1987, Kerwin et al 1987) or unsteady flows (Hsin 1990, Kinnas & Hsin 1992). The names of the corresponding codes are PSF-10 and PUF-10, respectively. In the case of non-axisymmetric inflows the trailing wake shape is assumed to be the same at all blade angles and is determined from alignment with the circumferentially averaged inflow.

2.3 Improved wake model in PUF-3A

The model described in Section 2.2 was recently implemented in PUF-3A (Pyo & Kinnas 1996). The corresponding code is called HPUF-3AL and also includes the effects of the hub on blade cavitation (Kinnas 1996). In this wake model the ultimate wake radius was first taken equal to 0.83 of the propeller radius. However, to avoid the inconsistency in PUF-3A (as described in Section 2.1) an ultimate wake radius equal to the propeller radius is considered. The original wake (default) and the aligned wake with two different ultimate wake radii are shown in Figure 3 for propeller DTMB 4661 (Boswell et al 1984).

The effect of the wake model on the predicted cavity shape can be seen in Figure 4. Note that the cavity extent and volume are not affected appreciably. The effect of the wake model on the predicted blade forces (in steady wetted flow) is shown in Table 1. Note that the current model underpredicts the forces substantially when the old wake model is employed in HPUF-3AL. In addition, the forces are not considerably altered when an ultimate wake radius of 1.0 instead of 0.83 of the propeller radius is considered.

WAKE MODEL	F_X	F_Y	F_Z
Old model	-0.07569	-0.01593	0.04692
Aligned (RULT=1)	-0.07945	-0.01649	0.04921
Aligned (RULT=0.83)	-0.07933	-0.01639	0.04905
PSF-10	-0.07852		

WAKE MODEL	Q_X	Q_Y	Q_Z
Old model	0.01651	0.00020	0.02585
Aligned (RULT=1)	0.01728	0.00031	0.02719
Aligned (RULT=0.83)	0.01725	0.00036	0.02720
PSF-10	0.01724		

Table 1: The steady fully wetted forces per blade. Predicted by HPUF-3AL with default and aligned wake models, and PSF-10 (with aligned wake model). Propeller DTMB 4661, $J_S = 0.8$.

2.4 Full wake alignment (with roll-up)

As mentioned in Section 2.2, the iterative lifting surface method for the wake alignment "artificially" suppresses the tip vortex roll-up.

The contraction of the wake (which is due to the mechanism of the roll-up) and the ultimate wake radius are parameters determined from experimental observations. The full wake alignment for propellers in non-uniform inflows was first treated by (Keenan 1989). He applied a vortex lattice method (VLM) on both blade and wake and was able to predict the gross characteristics of the wake geometry. However, due to inherent numerical instabilities when finer discretization is used or during late stages of the wake evolution, this method cannot predict the detailed structure of the wake roll-up.

In (Pyo 1995) and (Pyo & Kinnas 1997), an iterative process for the complete wake alignment, including roll-up, was introduced and implemented in the propeller panel method. This method was also coupled with the flow adapted grid, FLAG, introduced in (Kinnas et al 1993). The corresponding code is called PSF-10FLAG. The location where the tip vortex detaches from the blade is defined by the ratio AS/AT, as depicted in Figure 5. Panels with bi-quadratic dipole strength are utilized in order to model the wake surface and in particular the wake roll-up region. The method is capable of predicting the detailed structure of the wake roll-up in three dimensions as shown in Figure 8. The contraction of the wake and the ultimate wake radius are now evaluated by the method.

It should be noted that for some blade geometries and inflow conditions the predicted wake sheet roll-up may be sensitive to the number of panels in the wake, despite the high-order dipole panel representation. This has been attributed to the inadequacy of coarser grids to capture the slope of the blade loading at the tip, which in turn has been found to be very critical in evaluating the initial stage of the roll-up. In order to get sufficient representation of the roll-up during its initial stage a minimum number of panels has been found to be required in the wake (usually, 40 spanwise and 30 streamwise panels). In addition, the wake shape and induced velocities are re-splined after each roll-up iteration. These changes (described in more detail in Appendix A) were incorporated in PSF-10FLAG and were found to render reliable results over a wide range of blade geometries and advance

ratios.

The location of the tip detachment point can affect the results at the tip substantially. This is shown for example in Figure 6 where the pressure distribution on the blades of DTMB 5168 is shown for three different locations of the tip vortex detachment. Note that the pressure distribution everywhere on the blade (except at the tip) is unaffected by the detachment point. In this particular case $AS = 1.20AT$ appears to be the detachment point with the smallest region of singular regions at the tip. The corresponding blade and rolled-up wake grids are shown in Figure 7. More recently, a wake roll-up process based on the de-singularization of the tip vortex (Krasny 1987) was developed by (Ramsey 1996). In the case of wings a study of the tip vortex detachment location on the tip flow is described in Appendix B. Finally, the prediction of the viscous flow inside the core of a tip vortex is addressed in Appendix C.

2.5 Comparison with experiments

The predicted wake shape by PSF-10FLAG for DTMB 4119 is shown in Figure 8 to be very close to measured (Jessup 1989).

The predicted open water characteristics by different methods are shown together with the measured in Figure 9. The geometry and the open water measurements for DTMB 5168 were provided by (Jessup 1996). The geometry is also given in Appendix D. A friction coefficient of 0.0035 has been used on all methods. All methods seem to give very good predictions around design $0.8 < J_S < 1.2$. HPUF-3A-INC (same as HPUF-3AL for zero shaft inclination) appears to underpredict K_T for $J_S < 0.8$ and K_Q for $J_S > 1.2$. PSF-10[4] appears to underpredict the torque for $J_S > 1.2$. Finally, PSF-10FLAG, appears to predict forces closer to experiment for a wide range of $0.6 < J_S < 1.6$. The improvement in the K_Q predicted by PSF-10FLAG may be explained by the fact that the detachment point with the "smallest singular pressure region" was used in the calculation, and that the moment of the tip pressures with respect to the propeller axis can be appreciable. More investigation, including systematic observations of the location of the tip vortex detachment point, is needed to confirm our conjecture regarding the improved PSF-10FLAG predictions at high J's.

The rolled-up wake geometry predicted by PSF-10FLAG for $J_S = 0.6$ is shown in Figure 10. It should be noted that the wake is assumed to start at the propeller's tip ($AS/AT = 1$) without allowing for leading edge vortex separation which may be present at this low advance ratio. In regards to the stability of our method, as also mentioned in Section 2.4, a sufficient number of panels is needed in the spanwise direction in order to produce stable roll-ups.

[4]This version of PSF-10 uses a wake alignment scheme similar to that described in Section 2.2.

3 INCLINED INFLOW

3.1 Trailing wake geometry

A propeller subject to uniform inflow with inclination angle α is shown in Figure 11. This is equivalent[5] to having the propeller subject to uniform inflow with the shaft being inclined at an angle α (positive when the downstream part of the shaft is at a larger depth than the upstream part). The total inflow, V_{IN} may be decomposed into an axial component, $V_A = V_{IN}\cos\alpha$, and a vertical component, $V_y = V_{IN}\sin\alpha$, as also shown in Figure 11. Subsequently, V_y can be decomposed into a radial component, V_R, and a tangential component, V_T, given as:

$$V_R(\theta) = V_y\cos\theta = V_A\tan\alpha\cos\theta \tag{3}$$

$$V_T(\theta) = -V_y\sin\theta = -V_A\tan\alpha\sin\theta \tag{4}$$

The unsteady propeller flow in the presence of the uniform axial and the once per revolution varying radial and tangential inflows must be solved. As already mentioned in the introduction the alignment of the trailing wake for each blade angle is required in order to predict the blade forces accurately. Ideally, the trailing wake geometry could be determined at each blade angle by alignment with the local (time dependent) flow. Since this process is expected to be prohibitively computer intensive, a more efficient procedure is proposed in this paper. This procedure is depicted in Figures 12 and 13. The trailing wake geometry is determined as the superposition of (a) the trailing wake geometry for uniform axial inflow with zero inclination, and (b) an angular shift of the wake geometry equal to the angle of inclination. As a result of this superposition the trailing wake geometry will change with blade angle as shown is Figure 13. This approximation of the wake geometry is expected to be as accurate in inclined flows as the approximations involved in the method of (Greeley & Kerwin 1982) in straight inflows.

In Figure 11 the total velocity vector $\vec{V}_o$ (average of the flow velocities on the two sides of the wake sheet) on the trailing wake surface is shown with respect to a coordinates system rotating with the propeller. The axial, radial, and tangential components of the total velocity (shown in Figure 11) are given as follows:

$$V_o^A = V_A + u_a \tag{5}$$

$$V_o^R = V_R(\theta) \tag{6}$$

$$V_o^T = V_T(\theta) + u_t + \omega r \tag{7}$$

[5] We ignore the wake defect in the shadow of the inclined shaft.

where u_a and u_t are the axial and the circumferential components of the propeller induced perturbation velocity, respectively. These velocities are evaluated with the propeller subject only to the uniform axial inflow (i.e. at zero inclination angle). The method described in Section 2.2 is used at this stage. Note that the induced radial perturbation velocity is not included in V_o, since this component is not utilized in the wake alignment process, as explained in an earlier section.

The geometry of the transition wake is determined by starting at the trailing edge at each radial position and then advancing in constant increments $\Delta\theta$ in the circumferential direction. Usually $\Delta\theta = 6°$. The increments in terms of the edges of the panels in the trailing wake are given from the following equations. This is also depicted in Figure 11.

$$\Delta x = V_o^A \Delta t = \frac{V_A + u_a}{V_S}\left(J_S \frac{\Delta\theta}{180}\right) \tag{8}$$

$$\Delta y = \Delta R\cos\theta - \Delta T\sin\theta \tag{9}$$

$$\Delta z = \Delta R\sin\theta + \Delta T\cos\theta \tag{10}$$

where

$$\Delta t = \frac{\Delta\theta}{\omega} = \frac{J_S}{V_S}\frac{\Delta\theta}{180} \tag{11}$$

$$\Delta R = V_o^R \Delta t = \frac{V_R}{V_S}\left(J_S \frac{\Delta\theta}{180}\right) \tag{12}$$

$$\Delta T = V_o^T \Delta t = \left[\frac{V_T + u_t}{V_S} + \frac{\pi}{J_S}\right]\left(J_S \frac{\Delta\theta}{180}\right) \tag{13}$$

where α is the inclination angle, θ is the angular position in the wake of the blade, J_S is the advance coefficient, ω is a propeller angular velocity. In the ultimate wake region, the pitch is calculated in the same manner as in the uniform inflow case. The aligned wake geometries at three angular positions are also shown in Figure 14.

This wake model has been implemented in HPUF-3AL and the new version is called HPUF-3A-INC. The influence coefficients of the trailing wake vortex horse-shoes on the key blade are evaluated at each blade angle (60 in total). As a result the computing time is increasing considerably (about five times) when the inclined wake geometry is included. A 20×18 HPUF-3A-INC run on a DEC Alpha 600-5/266 takes about 15 minutes of CPU time when the inclined wake geometry is included.

3.2 Results

Results are presented next for propeller DTMB 4661 (Boswell et al 1984) the geometry of which is given in Appendix D.

First the effect of the inclined trailing wake geometry on the blade forces is shown in Figure 15. Note the considerable difference when the inclined wake geometry is included in the calculation. A similar effect was also reported in (Kerwin 1979).

Figures 16 and 17 show the effect of the inclined wake geometry on the predicted cavity shapes. The inclined wake model predicts a larger cavity extent.

Figures 18 and 19 show the predicted cavity volume for: (a) straight trailing wake and by considering only the axial inflow component, (b) same as a) by also adding the radial component, (c) same as b) by also adding the tangential component and (d) inclined trailing wake with all inflow components. Note the expected negligible effect of the radial component on the predicted cavity volume. The inclusion of the tangential component in the inflow changes the value and the angular location of the maximum cavity volume drastically. This is due to an increase of the local angle of attack at 90^o and a decrease of the local flow angle at 270^o, when the tangential inflow component is considered. Finally, the cavity volume increases even more when the inclined wake model is included. This increase is consistent with the already shown increase in the blade forces.

Figures 20 and 21 show the amplitudes of the first harmonic of the forces acting on the blades of propeller DTMB 4661 for two inclination angles and over a range of advance ratios. The measured forces (Boswell et al 1984) are shown together with those predicted by the present method and the method in (Kerwin 1979) where the inclined wake geometry is considered at blade angles of 0^o, 90^o, 180^o and 270^o. Note the fair agreement of the predictions from both methods with the measurements. The present method, however, incorporates a more complete inclined wake model (which may be necessary for propeller geometries or inclinations other than those presented in Figures 20 and 21), and most importantly, includes the modeling of cavitation.

4 CONCLUSIONS

Existing trailing wake models are reviewed and the predicted open water characteristics are compared again each other and against experimental measurements. While the more sophisticated models can predict wake shapes and pressure distributions at the blade tip more accurately than the simpler, all models seem to predict the forces within acceptable accuracy, especially in the range of design J.

One of the simpler models is extended in the case of cavitating flow in inclined inflow. The geometry of the inclined wake is calculated at all blade angles. The effect of the inclined wake on the predicted cavity volume and unsteady blade forces is found to be significant. The predicted forces compare well to those measured in inclined shaft propeller experiments.

5 ACKNOWLEDGMENTS

Support for this research was provided by the Office of Naval Research (Contract number N00014-96-1-0231, Monitors: Dr. Peter Majumdar and Dr. Edwin Rood) and by a Consortium on Cavitation Performance of High Speed Propulsors.

REFERENCES

BOSWELL, R., JESSUP, S., KIM, K. AND DAHMER, D. 1984 Single-Blade Loads on Propellers in Inclined and Axial Flows. Technical report. DTNSRDC-84/084. DTNSRDC. November.

GREELEY, D. AND KERWIN, J. 1982 Numerical methods for propeller design and analysis in steady flow. *Trans. SNAME*, **vol 90**.

HOSHINO, T. 1991 Numerical and experimental analysis of propeller wake by using a surface panel method and a 3-component LDV. *Proceedings:* Eighteenth Symposium on Naval Hydrodynamics (1990). National Academy Press, Washigton D.C., 297–317.

HSIN, C.-Y. 1990 Development and analysis of panel method for propellers in unsteady flow. Doctoral dissertation, Department of Ocean Engineering, MIT. September.

JESSUP, S. 1996 private communication.

JESSUP, S. 1989 An experimental investigation of viscous aspects of propeller blade flow. Doctoral dissertation, The Catholic University of America.

KEENAN, D. P. 1989 Marine propellers in unsteady flow. Doctoral dissertation, M.I.T., Department of Ocean Engineering. May.

KERWIN, J. 1979 The Effect of Trailing Vortex Asymmetry on Unsteady Propeller Blade Forces. Technical report. Department of Ocean Engineering, MIT.

KERWIN, J. AND LEE, C.-S. 1978 Prediction of steady and unsteady marine propeller performance by numerical lifting-surface theory. *Trans. SNAME*, **vol 86**.

KERWIN, J., KINNAS, S., WILSON, M. AND J., M. 1986 Experimental and analytical techniques for the study of unsteady propeller sheet cavitation. *Proceedings:* Proceedings of the Sixteenth Symposium on Naval Hydrodynamics. July.

KERWIN, J., KINNAS, S., LEE, J.-T. AND SHIH, W.-Z. 1987 A surface panel method for the hydrodynamic analysis of ducted propellers. *Trans. SNAME*, **95**.

KINNAS, S. 1983 A numerical method for the analysis of cavitating propellers in a nonuniform flow, mit-puf-3 program documentation. Technical report. 83-7. MIT, Department of Ocean Engineering. June.

KINNAS, S. 1991 Leading-edge corrections to the linear theory of partially cavitating hydrofoils. *Journal of Ship Research*, **35**, 1, March, pp. 15–27.

KINNAS, S. 1996 An international consortium on high-speed propulsion. *Marine Technology*, **33**, 3, July, pp. 203–210.

KINNAS, S. AND HSIN, C.-Y. 1992 A boundary element method for the analysis of the unsteady flow around extreme propeller geometries. *AIAA Journal*, **30**, 3, March, 688–696.

KINNAS, S., PYO, S., HSIN, C.-Y. AND KERWIN, J. 1993 Numerical modelling of propeller tip flows. *Proceedings:* Sixth International Conference on Numerical Ship Hydrodynamics. August, 531–544.

KRASNY, R. 1987 Computation of vortex sheet roll-up in the Trefftz plane. *Journal of Fluid Mechanics*, **184**, pp. 123–155.

LEE, C.-S. 1979 Prediction of steady and unsteady performance of marine propellers with or without cavitation by numerical lifting surface theory. Doctoral dissertation, M.I.T., Department of Ocean Engineering. May.

LEE, J.-T. 1987 A potential based panel method for the analysis of marine propellers in steady flow. Doctoral dissertation, M.I.T., Department of Ocean Engineering. August.

LOUKAKIS, T. A. 1971 A new theory for the wake of marine propellers. Technical report. 71-1. Dept. of Naval Architecture and Marine Engineering, Massachusetts Institute of Technology. May.

MORINO, L. AND BHARADVAJ, B. 1988 A unified approach for potential and viscous free-wake analysis of helicopter rotors. *Vertica*, **vol 12**, no 1/2.

PYO, S. 1995 Numerical modeling of propeller tip flows with wake sheet roll-up in three dimensions. Doctoral dissertation, M.I.T., Department of Ocean Engineering. July.

PYO, S. AND KINNAS, S. 1996 User's manual for HPUF-3AL (cavitating propeller analysis with wake alignment). Technical report. Ocean Engineering Group, UT Austin. April.

PYO, S. AND KINNAS, S. 1997 Propeller wake sheet roll-up modeling in three dimensions. *Journal of Ship Research*, **41**, 2, June, pp. 81–92.

RAMSEY, W. 1996 Boundary integral methods for lifting bodies with vortex wakes. Doctoral dissertation, M.I.T., Department of Ocean Engineering. May.

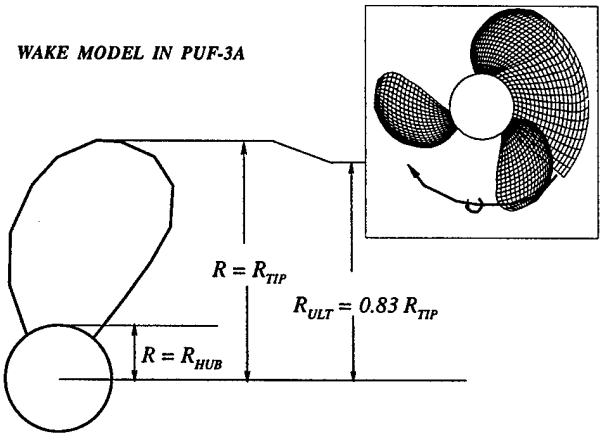

Figure 1: Partially aligned wake model in PUF-3A (original version).

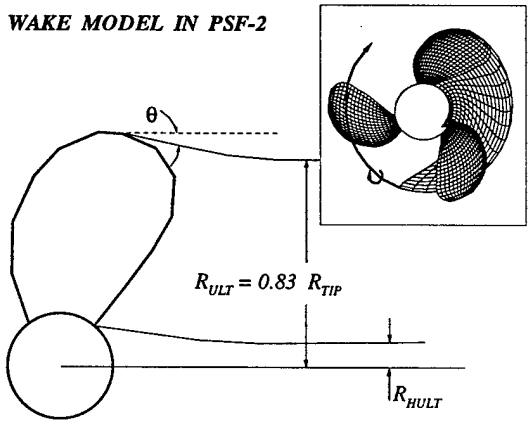

Figure 2: Aligned wake model in PSF-2.

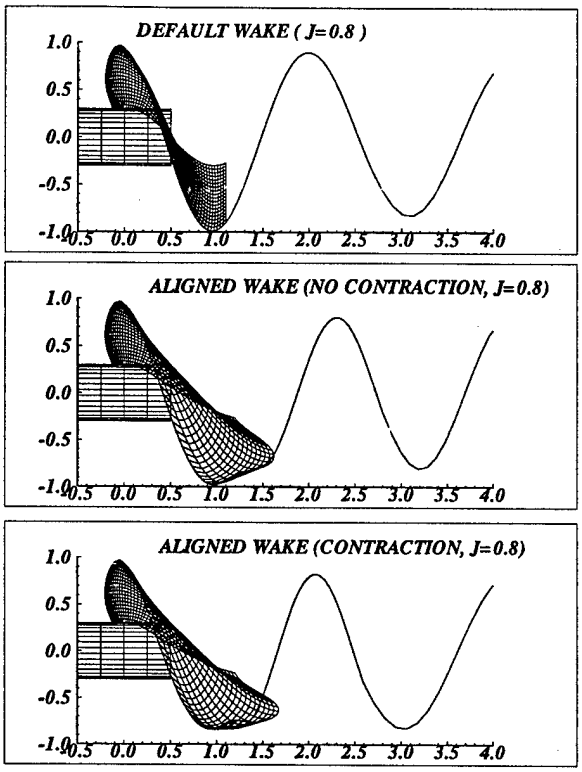

Figure 3: The default and the aligned wake models in HPUF-3AL; propeller DTMB 4661 at $J_S = 0.8$.

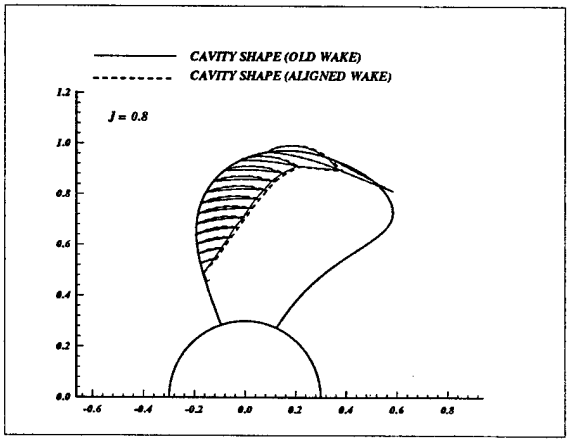

Figure 4: The cavity shapes predicted from HPUF-3AL with the default (old) and the aligned wake model. Propeller DTMB 4661, $J_S = 0.8, \sigma_n = 3.0, F_n = 10, \theta_B = 0^o$, uniform inflow.

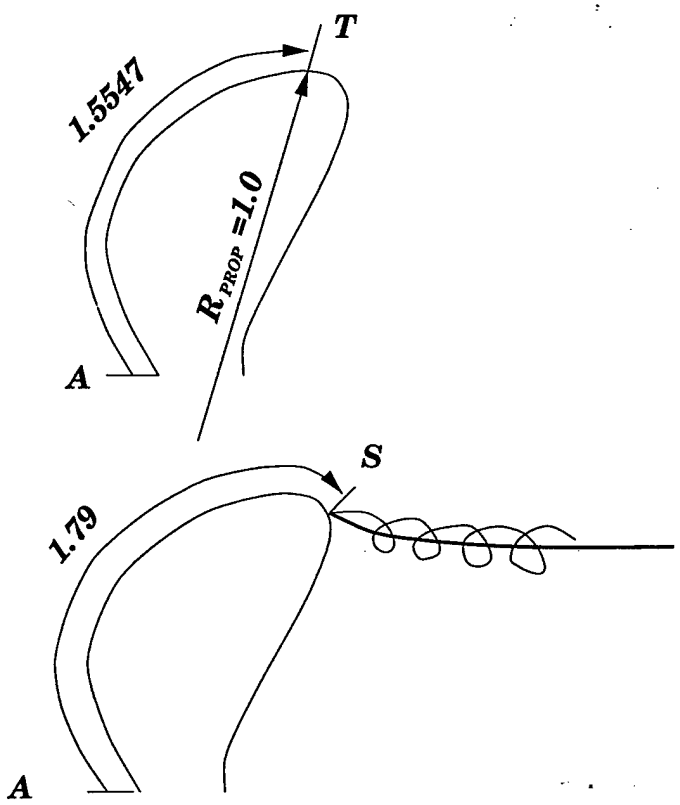

Figure 5: Definition of the arclengths AS and AT along the leading edge line; T is the propeller tip (point with maximum radius on the blade) and S is the specified tip vortex detachment point.

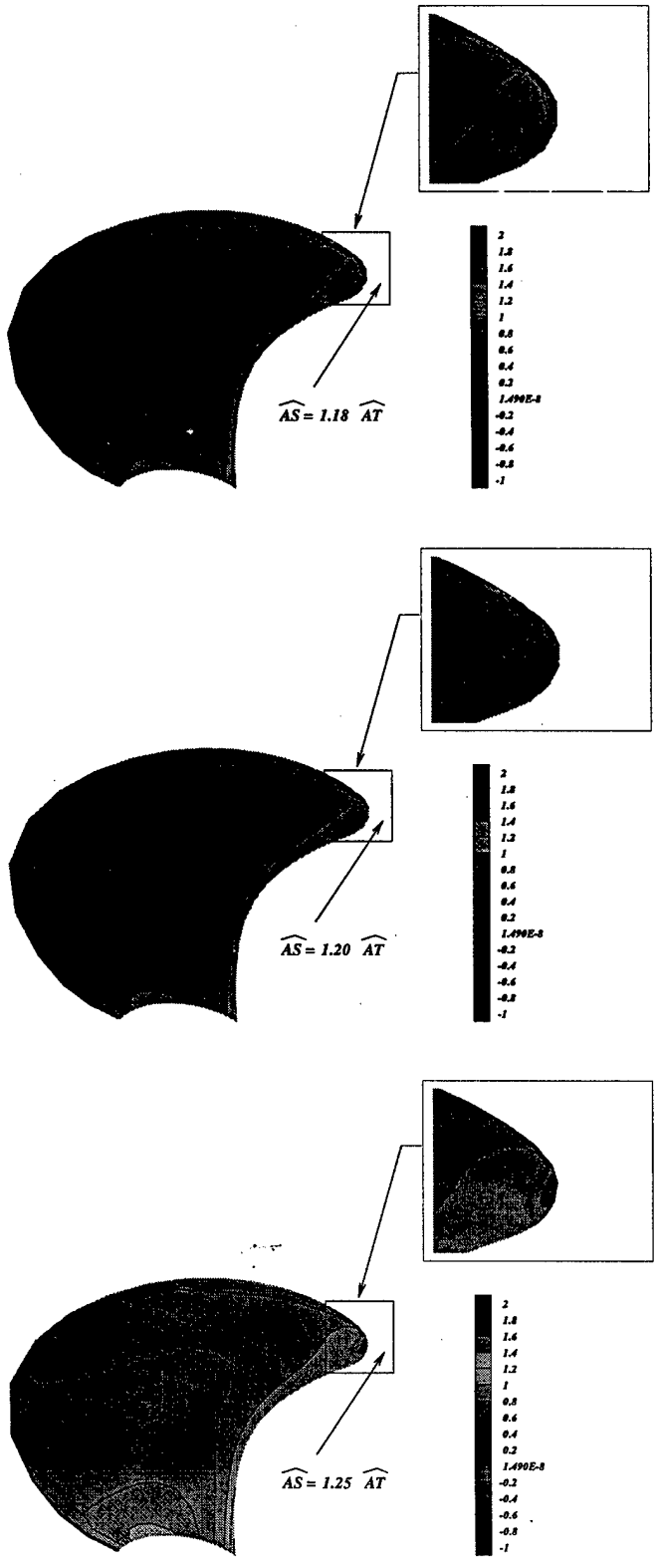

Figure 6: Pressure distribution ($-C_p$) for different locations of the tip vortex detachment point as predicted by PSF-10FLAG; propeller DTMB 5168 at $J_S = 1$.

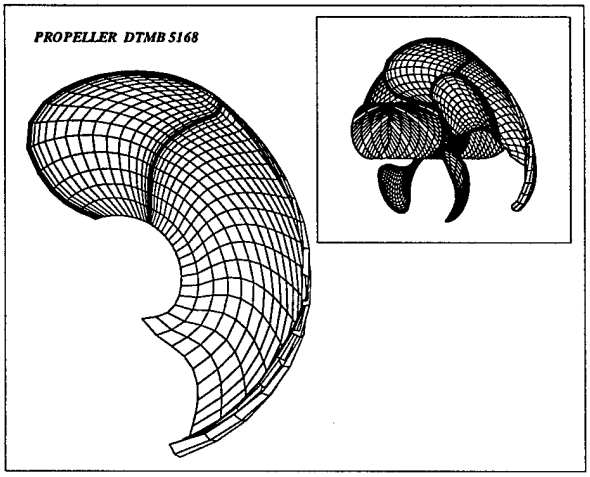

Figure 7: Fully aligned wake model in PSF-10FLAG. Propeller DTMB 5168 at $J_S = 1.0$.

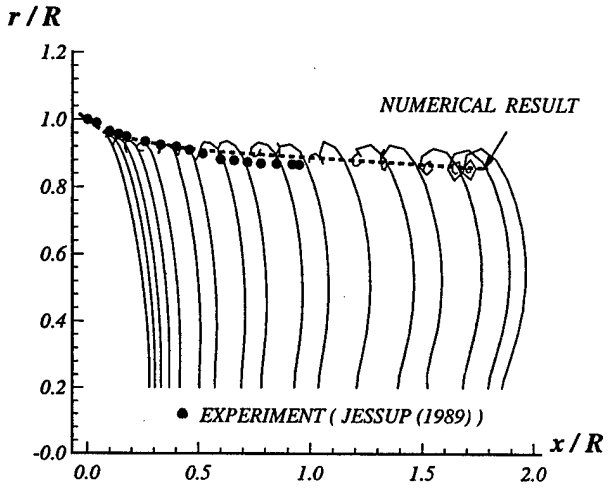

Figure 8: Radial location of the tip vortex for propeller DTMB 4119. From Pyo and Kinnas (1997).

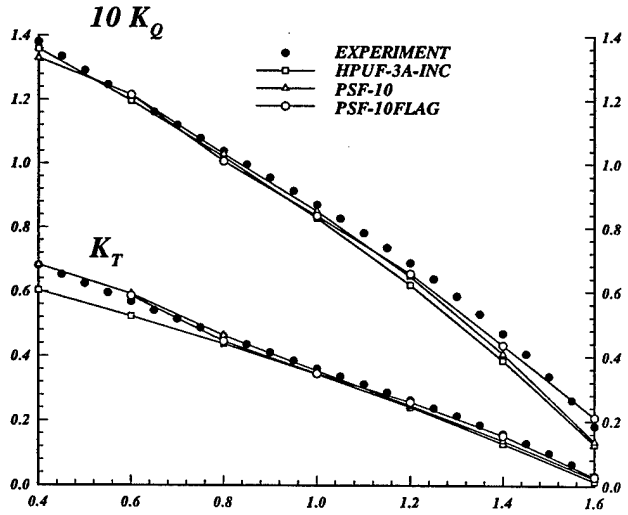

Figure 9: K_T&$10K_Q$ vs. J_S for propeller DTMB 5168; measured and predicted by different methods.

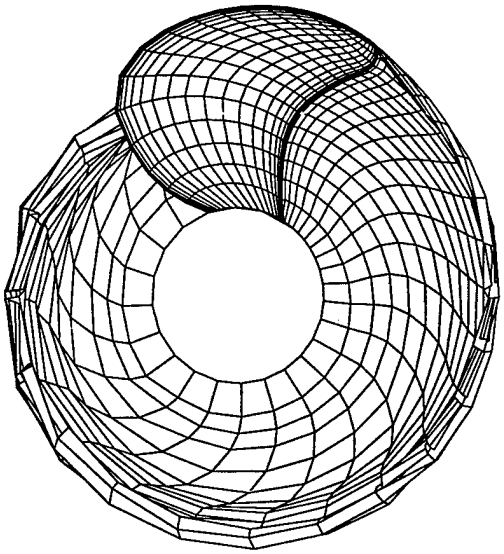

Figure 10: Wake geometry aligned using *PSF-10FLAG*. Propeller DTMB 5168 at $J_S = 0.6$.

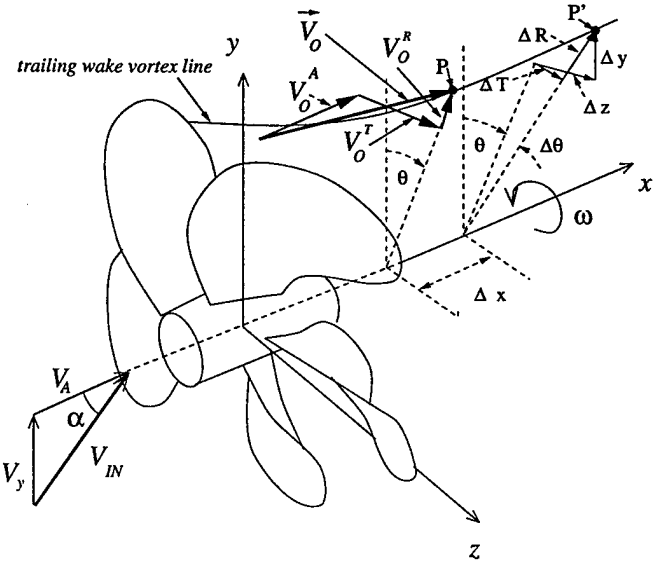

Figure 11: A propeller subject to uniform inflow with inclination α and the geometry of the inclined trailing wake geometry.

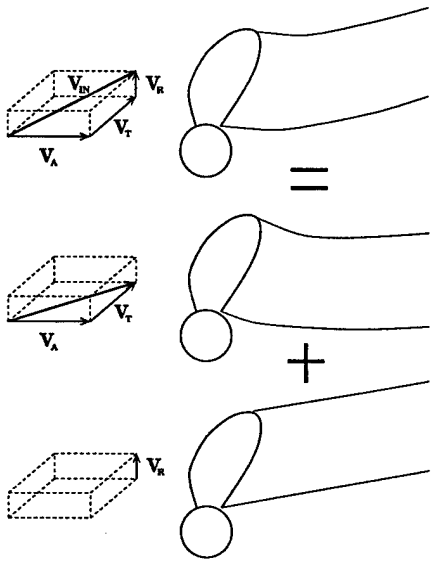

Figure 12: The principle behind the inclined flow wake model in HPUF-3A.

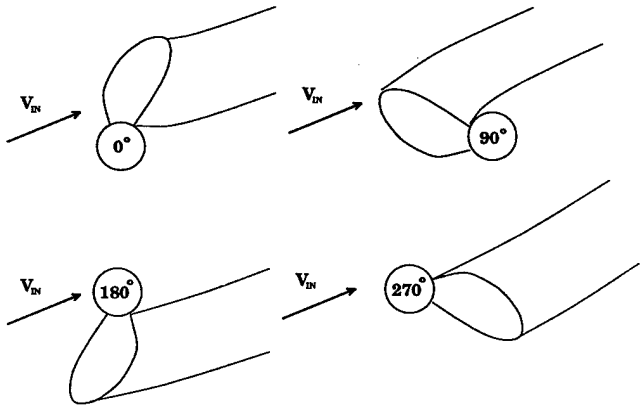

Figure 13: The key blade and its trailing wake geometry in inclined flow at three different blade angles.

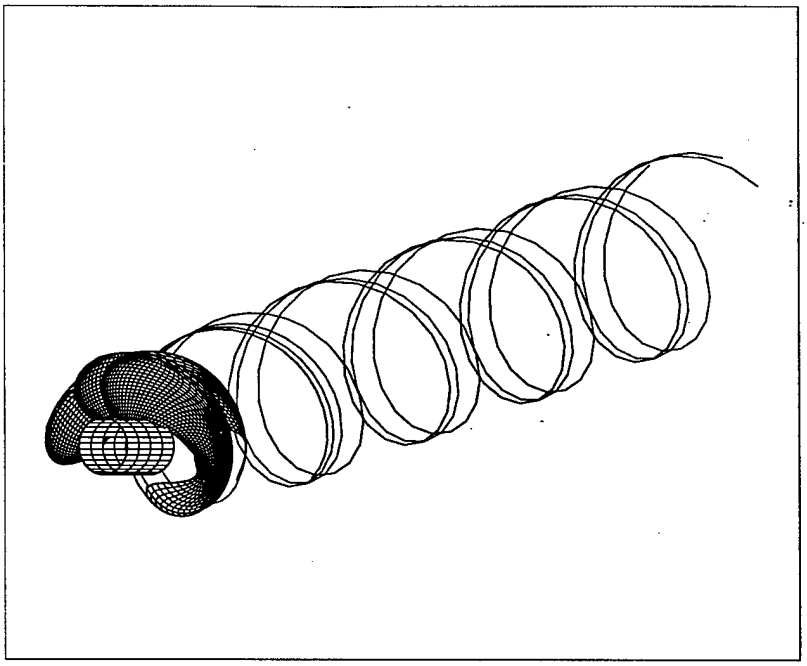

Figure 14: The trailing wake geometry aligned with the inclined flow shown at three angular positions; $\alpha = 20°$.

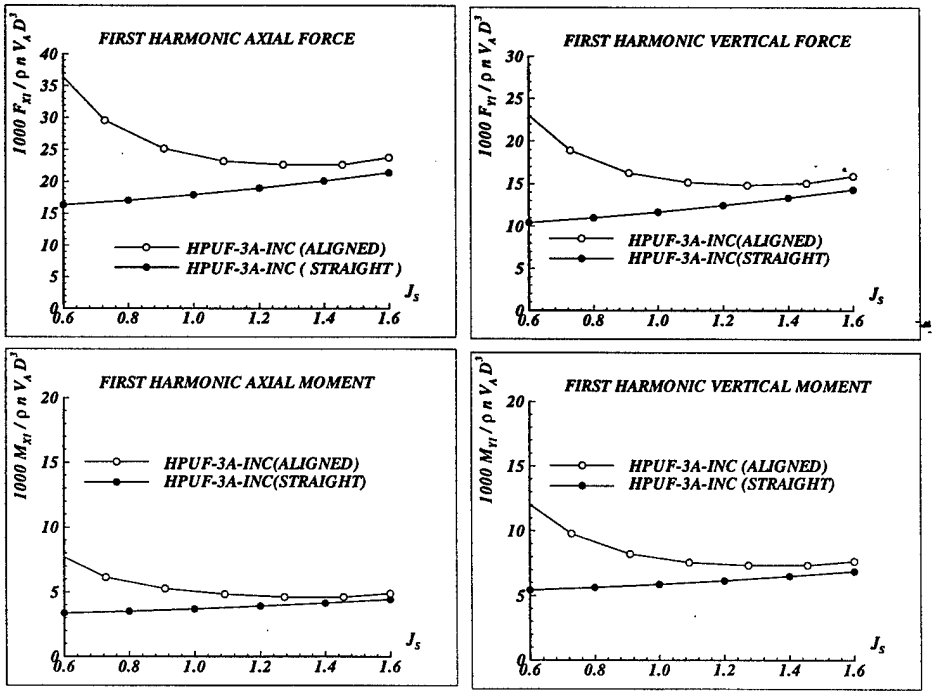

Figure 15: The first harmonic of the forces and moments acting on one blade for 10° shaft inclination; predicted by the present method with straight and inclined trailing wake. Propeller DTMB 4661, fully wetted flow.

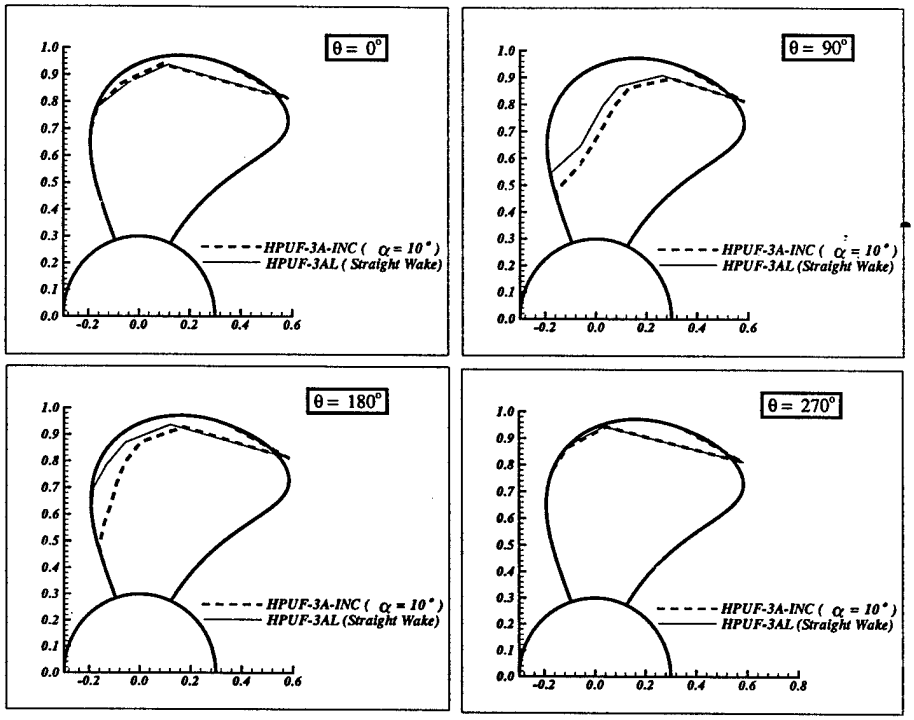

Figure 16: The cavity shape at four angular positions for 10° shaft inclination; predicted by HPUF-3AL (straight aligned wake) and HPUF-3A-INC (inclined aligned wake). Propeller DTMB 4661, $J_S = 1.0, \sigma = 0.2, F_n = 1.165$.

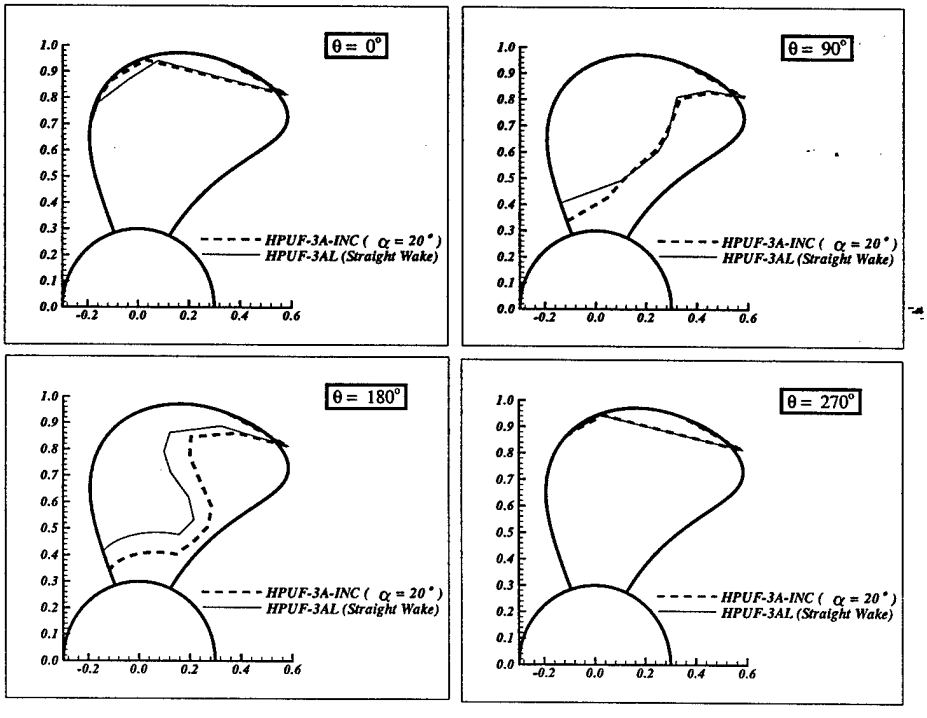

Figure 17: The cavity shape at four angular positions for 20° shaft inclination; predicted by HPUF-3AL (straight aligned wake) and HPUF-3A-INC (inclined aligned wake). Propeller DTMB 4661, $J_S = 1.0, \sigma = 0.2, F_n = 1.165$.

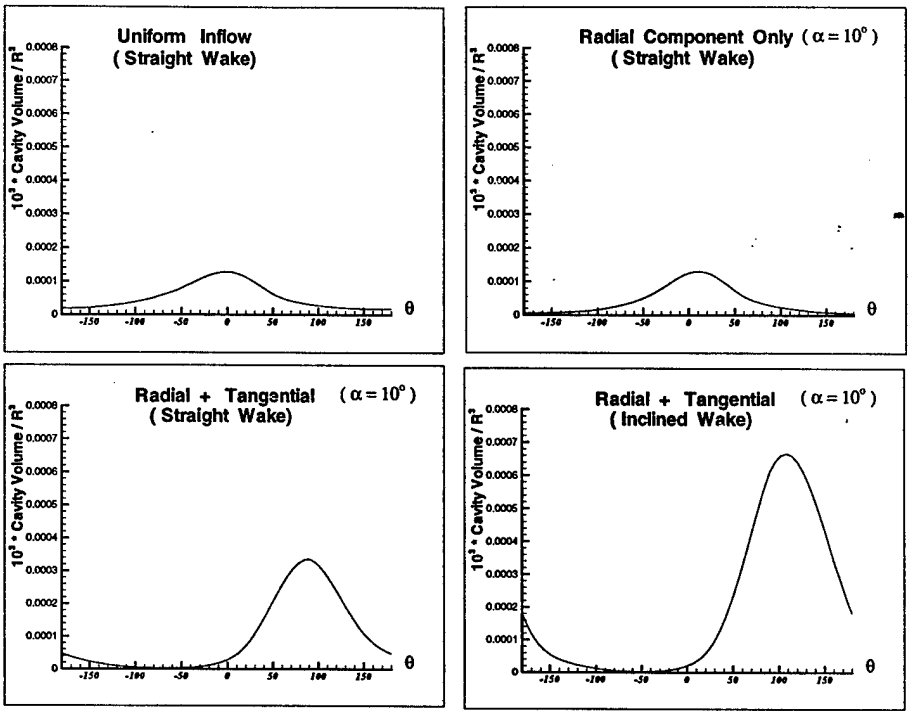

Figure 18: The cavity volume as a function of the blade angle for 10° shaft inclination; predicted by HPUF-3A-INC for different inflows and trailing wake geometries. Propeller DTMB 4661, $J_S = 1.0, \sigma = 0.2, F_n = 1.165$.

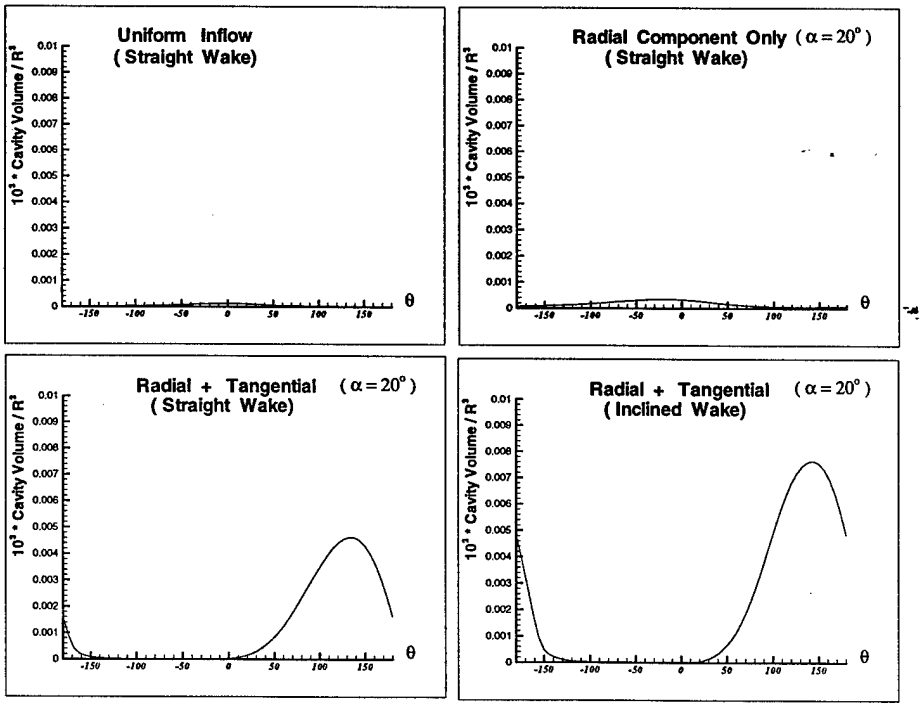

Figure 19: The cavity volume as a function of the blade angle for 20° shaft inclination; predicted by HPUF-3A-INC for different inflows and trailing wake geometries. Propeller DTMB 4661, $J_S = 1.0, \sigma = 0.2, F_n = 1.165$.

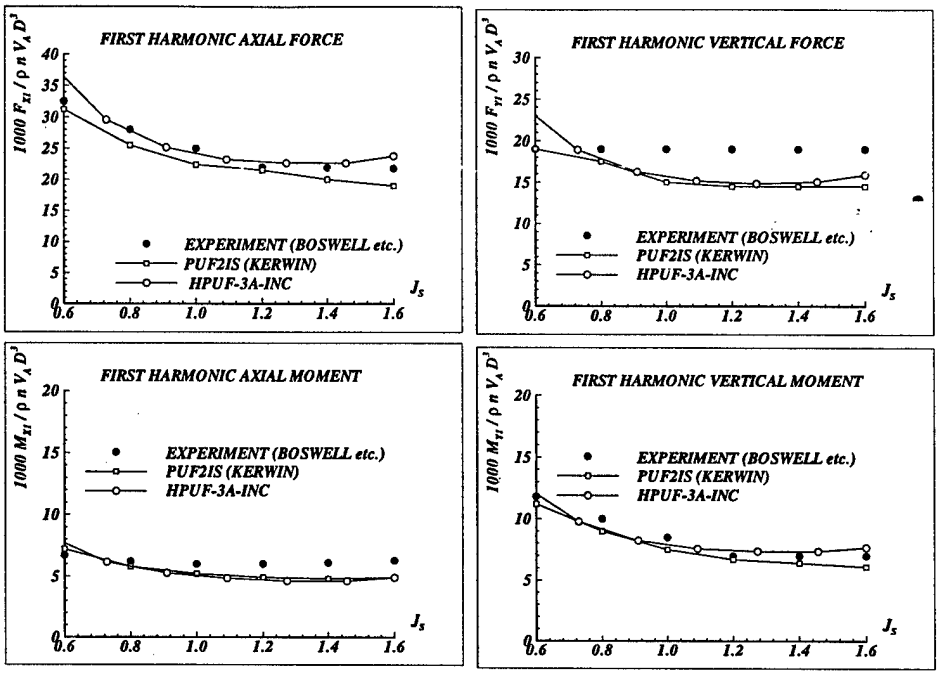

Figure 20: The first harmonic of the forces and moments acting on one blade for 10° shaft inclination; measured and predicted by the present (HPUF-3A-INC) and a previous method (PUF-2IS). Propeller DTMB 4661 in fully wetted flow.

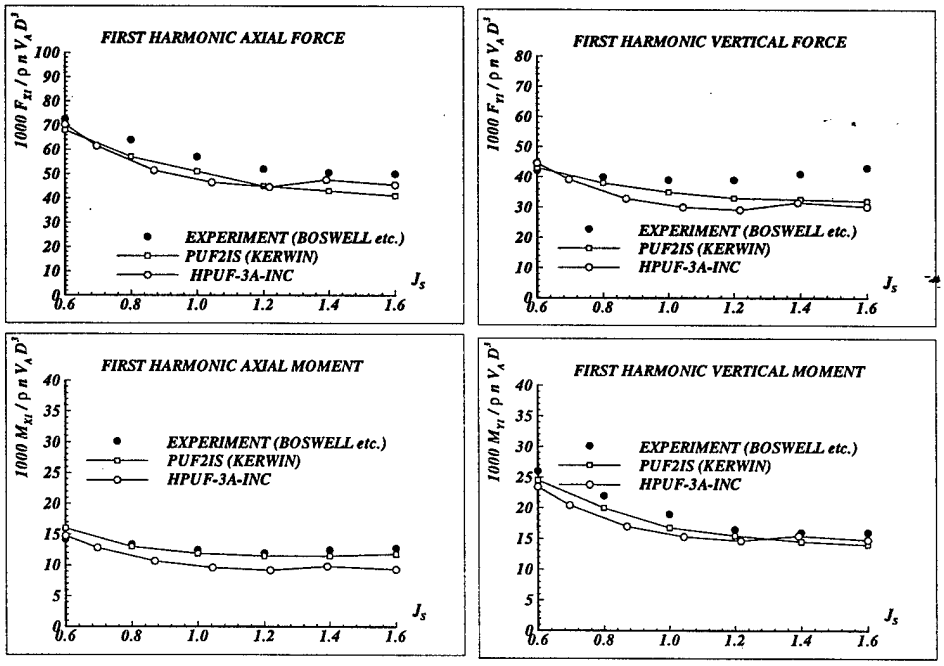

Figure 21: The first harmonic of the forces and moments acting on one blade for 20° shaft inclination; predicted by the present (HPUF-3A-INC) and a previous method (PUF-2IS). Propeller DTMB 4661 in fully wetted flow.

A The algorithm of the wake alignment model

III. ALIGNED WAKE MODEL WITH ROLL-UP

- PROCEDURE

(1) FIRST ITERATION

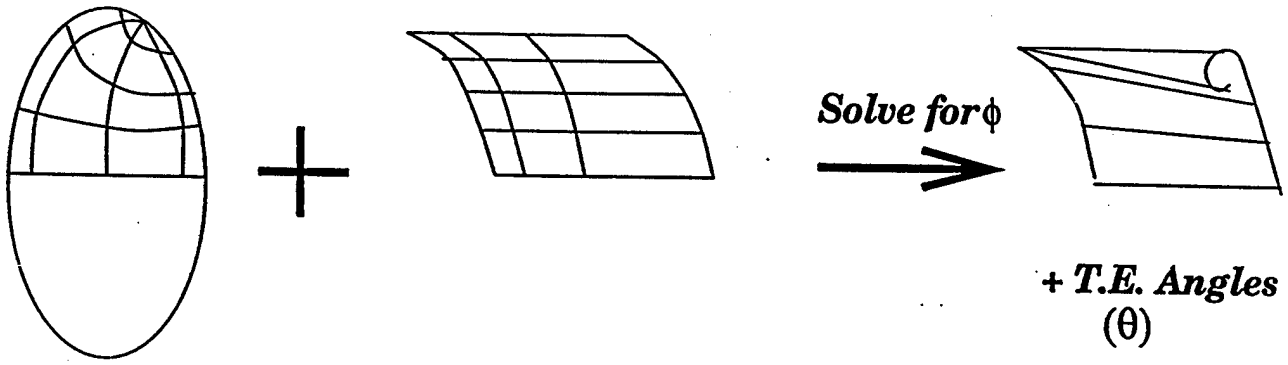

(2) SECOND & MORE ITERATIONS

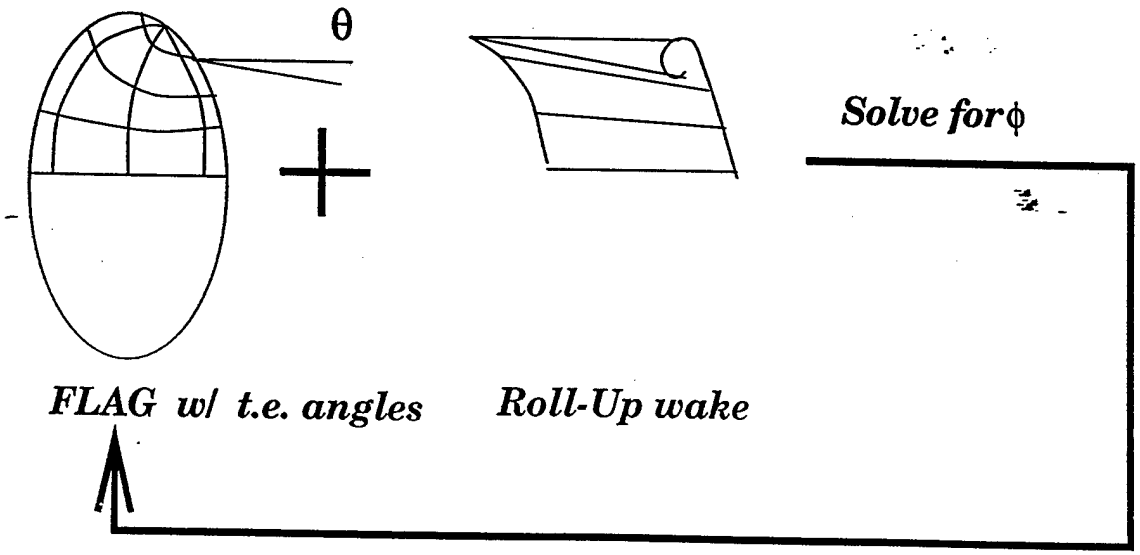

(b) IMPROVEMENT ON LOADING & FORCE CALCULATION.

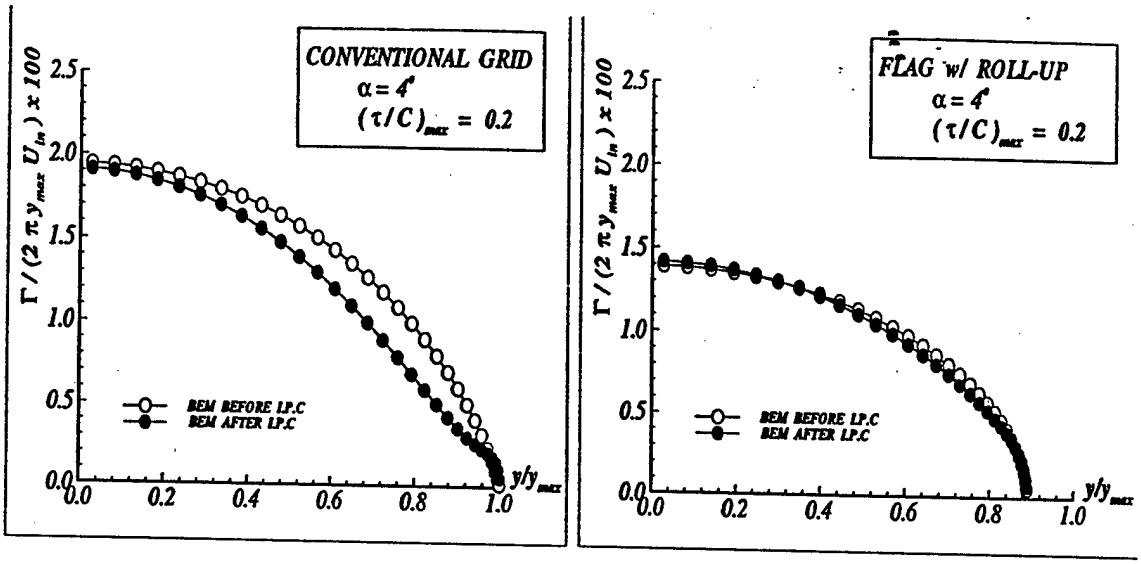

→ DIFFERENCE BETWEEN BEFORE I.P.C. AND AFTER I.P.C. BECOMES SMALLER.

→ FAST CONVERGENCE ON I.P.C.

IV. NUMERICAL RESULTS

- CIRCULAR PLANFORM WING
  - (a) MORE STABLE & RELIABLE PREDICTION ON THE SHAPE OF TRAILING WAKE SHEET ROLL-UP.

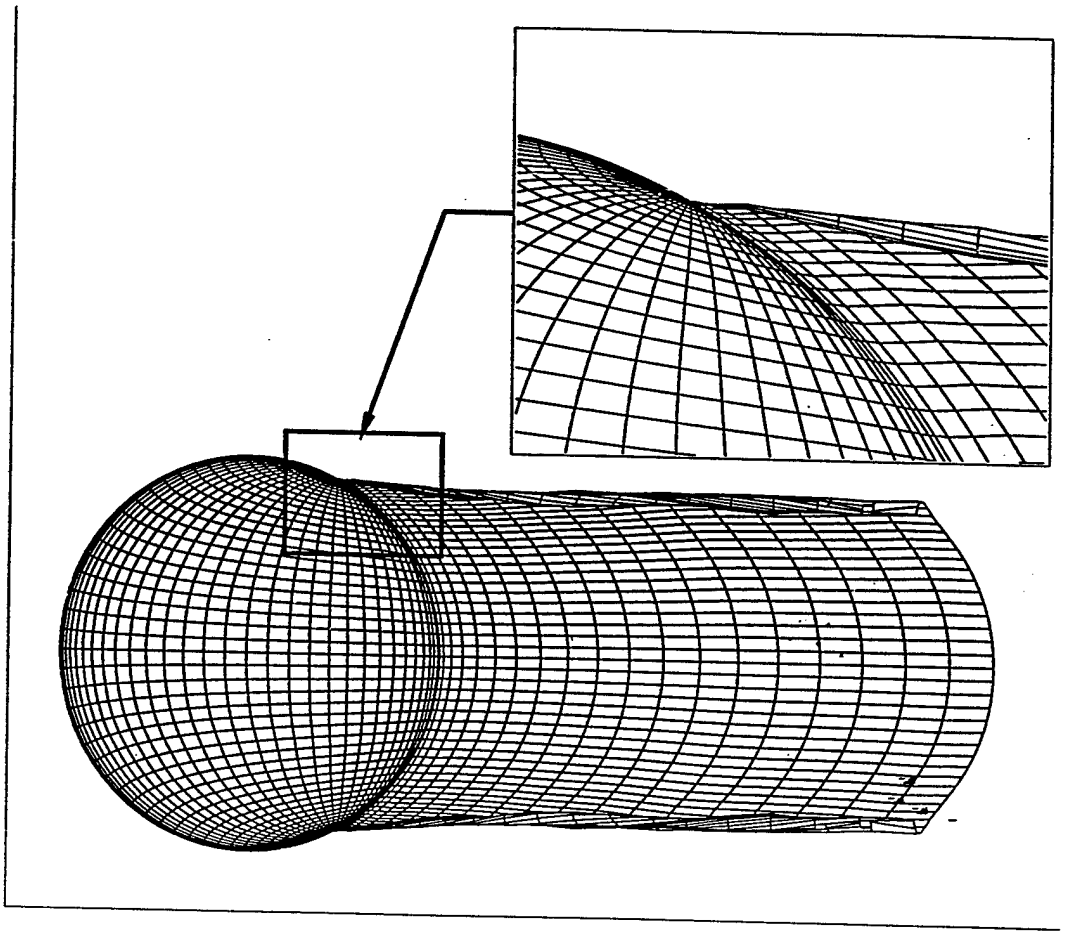

- ON THE BLADE
  - (a) B-SPLINE CURVE WITH GIVEN ANGLE AT THE TRAILING EDGE & NORMAL TO L.E..
  - (b) HALF COSINE SPACING ALONG SPANWISE DIRECTION & COSINE SPACING ALONG CHORDWISE DIRECTION.
  - (c) TWO SAME SIZE PANELS AT THE TAILING EDGE.
  - (d) GET TRAILING EDGE ANGLE FROM VELOCITY OF THE T.E. PANEL ON THE BLADE.

- IN THE WAKE
  - (a) HIGH ORDER PANEL METHOD WITH REDISCRETIZATION
  - (b) FIXED NUMBER OF PANELS (20×30)
  - (c) HALF COSINE SPACING ALONG STREAMWISE DIRECTION & COSINE SPACING ALONG SPANWISE DIRECTION.

B Effect of detachment location on tip flow for wings

DEFINITION OF TIP VORTEX DETACHMENT POINTS

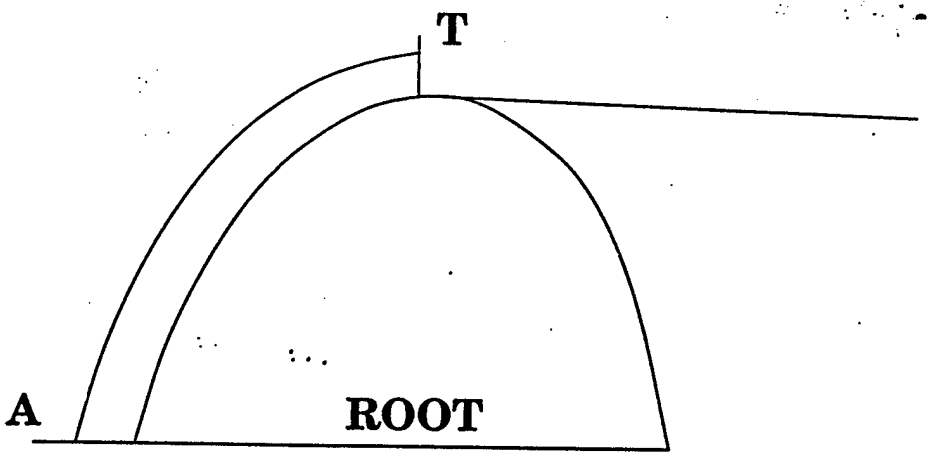

S = T, S at ratio 1.00

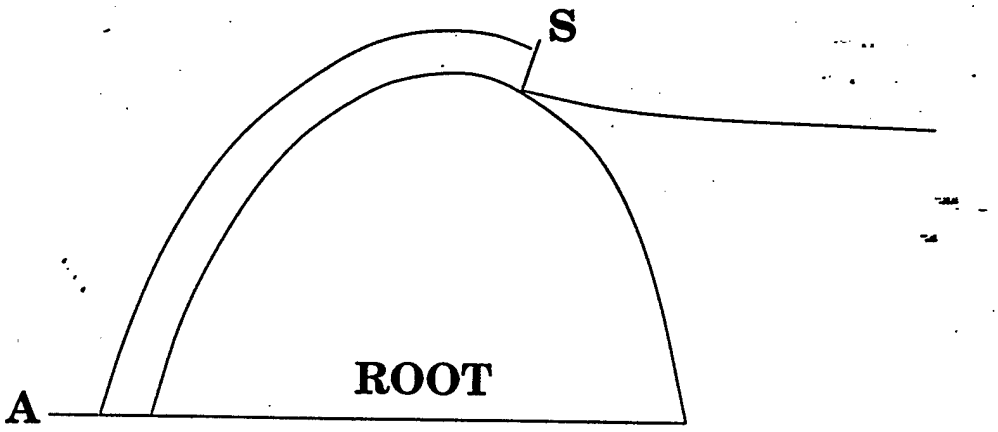

S at x : $\widehat{AS} = \frac{x}{100} \widehat{AT}$

1) Effect of detachment point on wake shape at the tip/TE for thin wings. (t/c = 2%, 6° angle of attack)

1.00

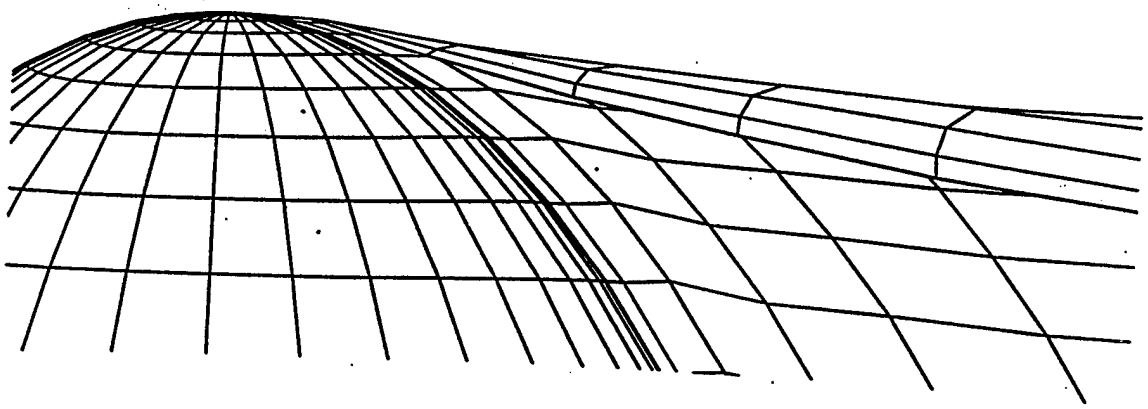

1.02

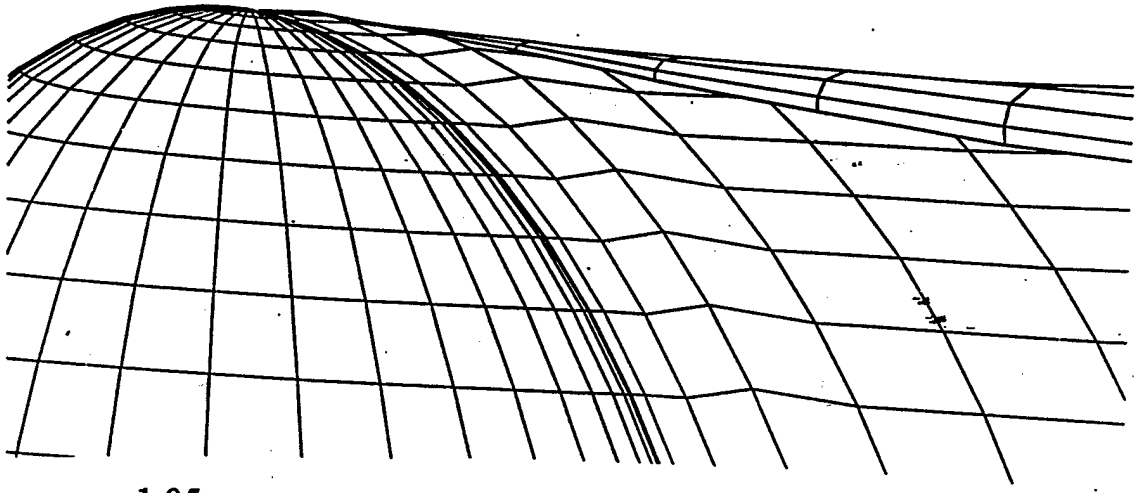

1.05

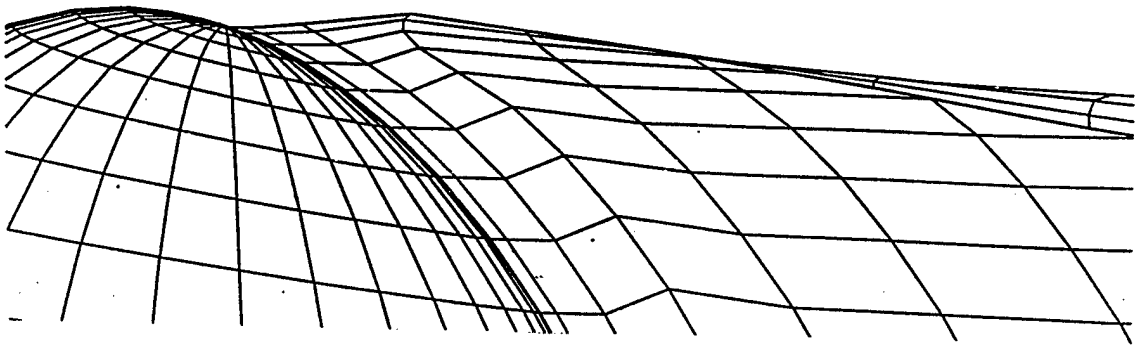

1) Effect of detachment point on wake shape at the tip/TE for thick wings. (t/c = 20%, 6° angle of attack)

1.00

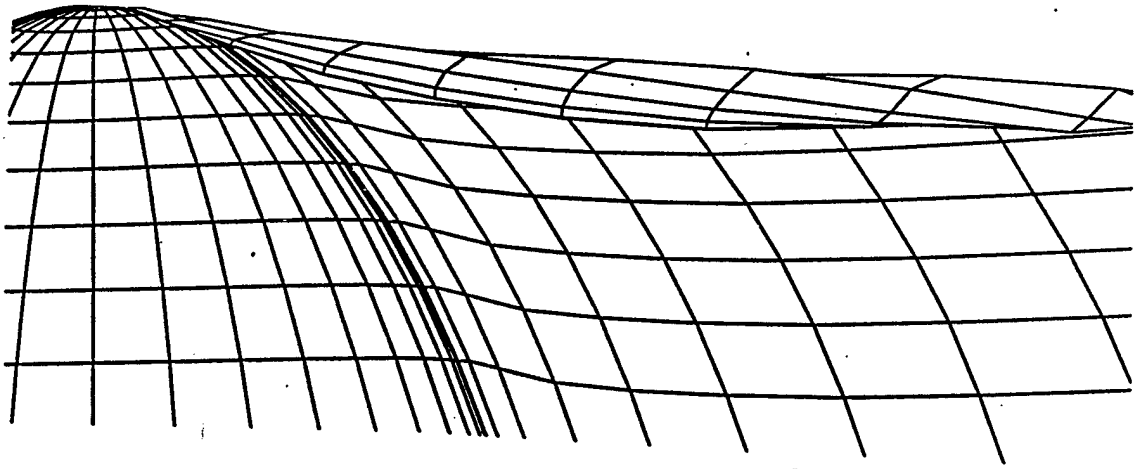

1.02

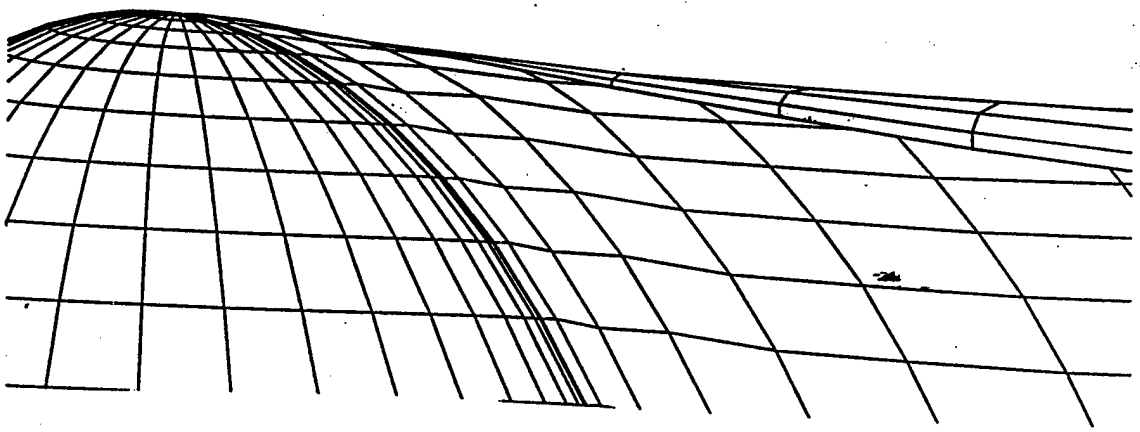

1.05

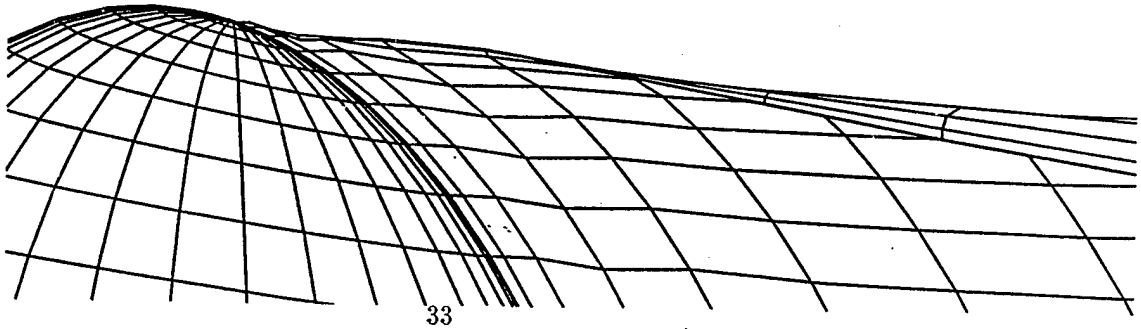

1) Effect of detachment point on wake shape at the tip/TE for thick wings. (t/c = 20%, 10° angle of attack)

1.00

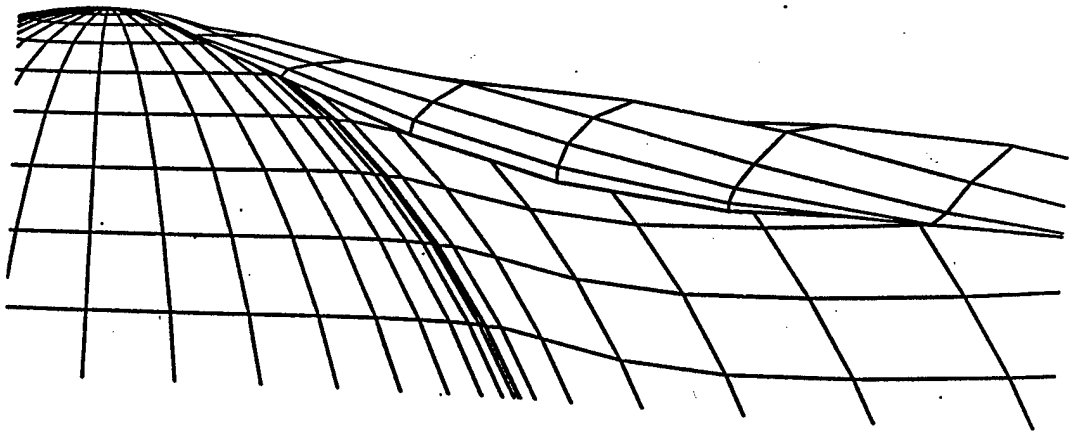

1.02

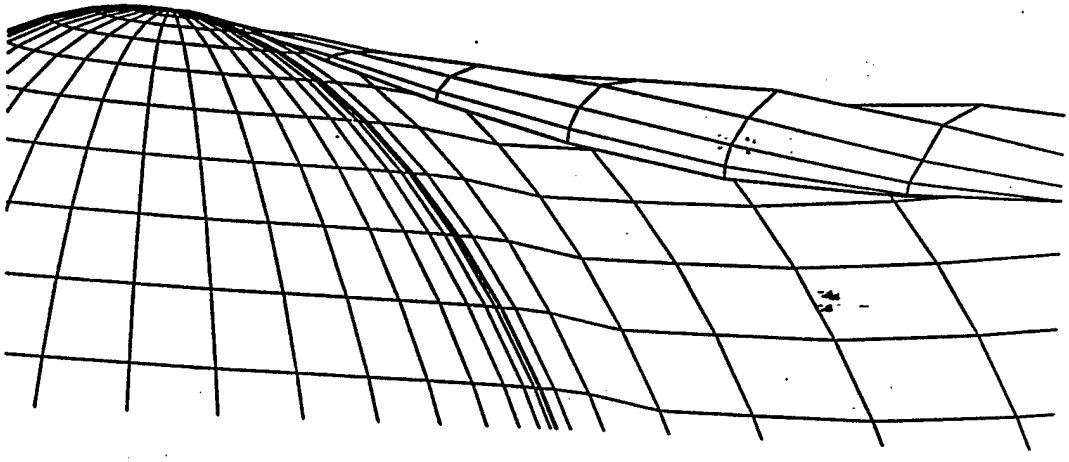

1.05

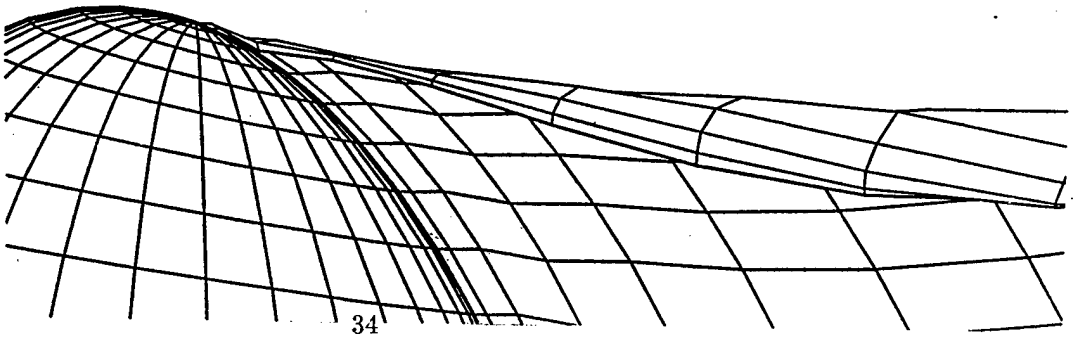

2) Effect of detachment point on pressure distribution (t/c = 20%, 6° angle of attack)

SUCTION SIDE

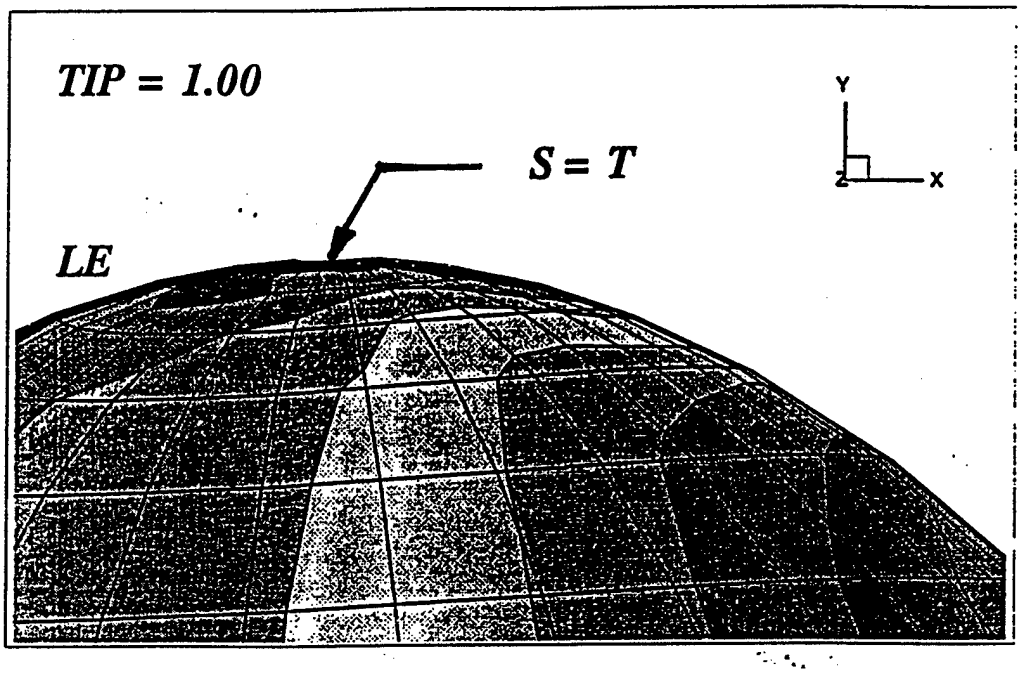

PRESSURE SIDE

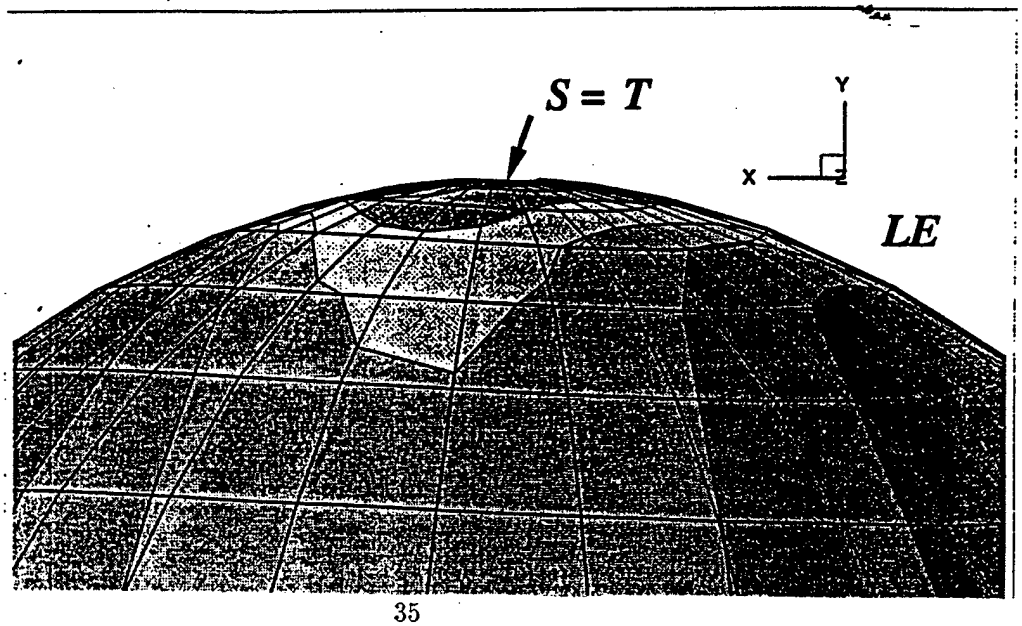

SUCTION SIDE

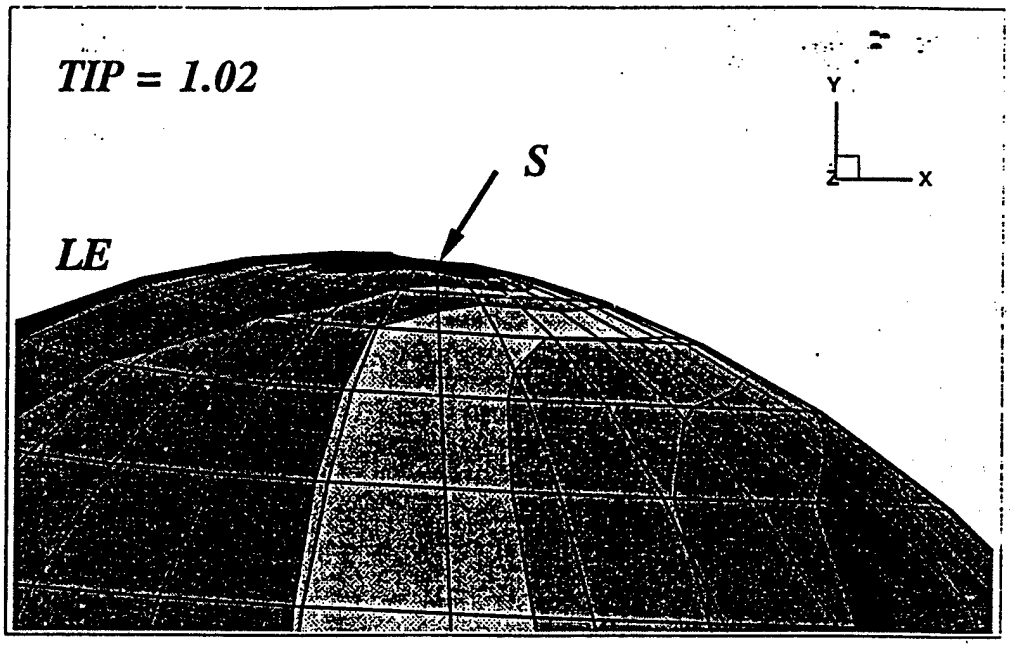

PRESSURE SIDE

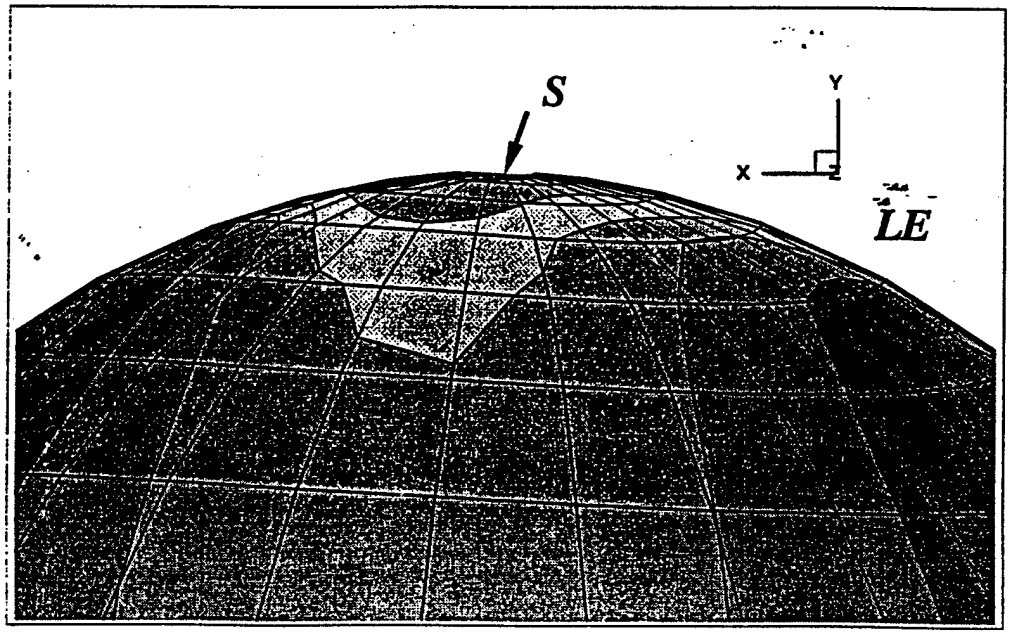

SUCTION SIDE

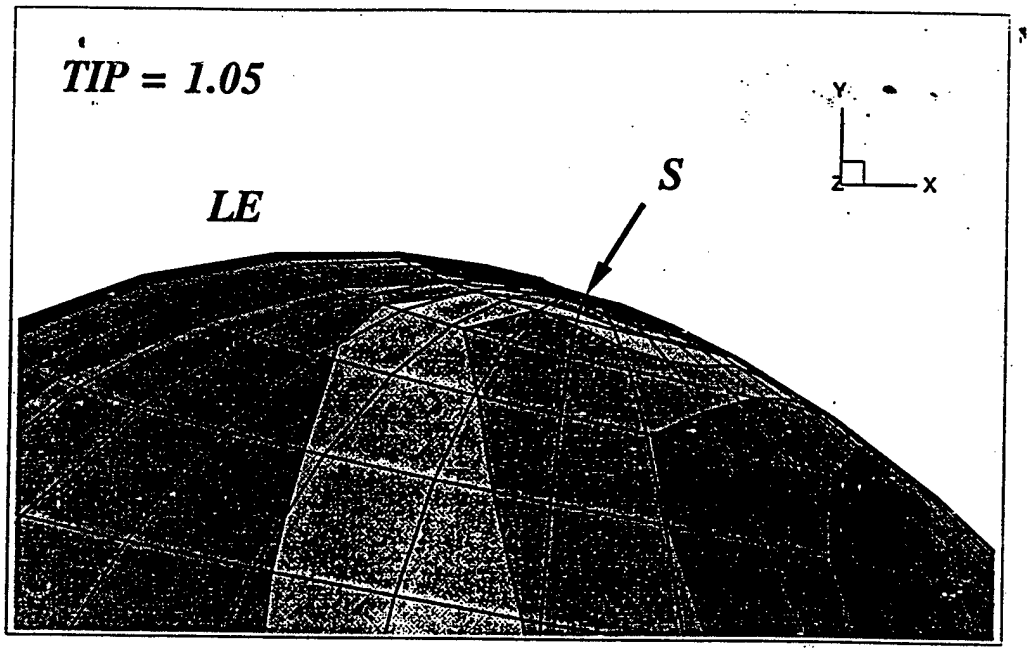

PRESSURE SIDE

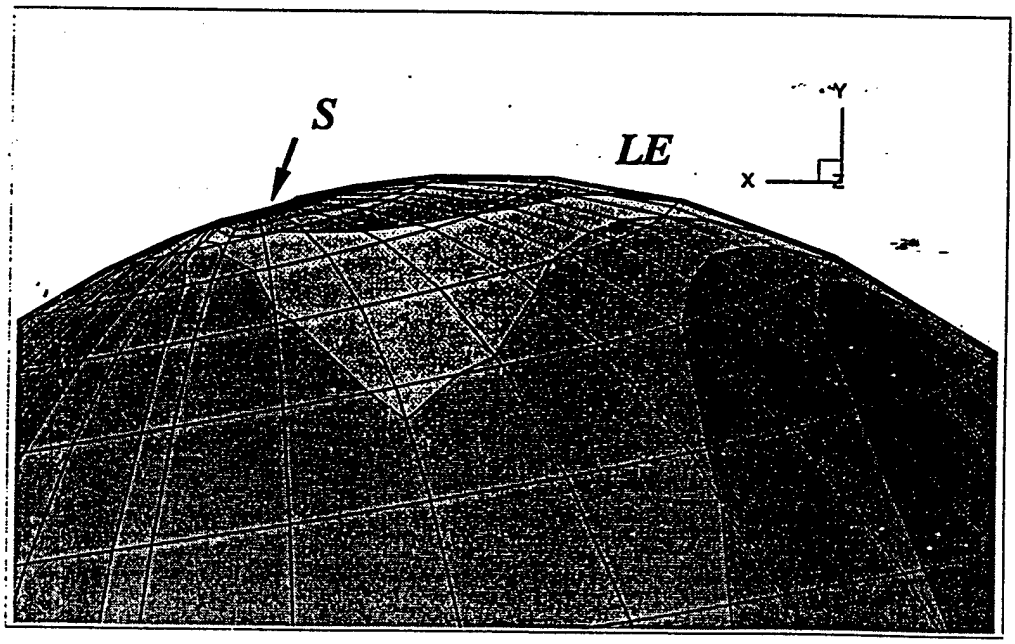

C Local viscous flow inside of a tip vortex

V. VISCOUS EFFECT INSIDE THE CORE

1. FORMULATION

- ASSUMPTION : SLENDER CORE & STEADY & AXISYMMETRY
- GOVERNING EQUATION

$$
\begin{aligned}
u\frac{\partial(rv)}{\partial x} + w\frac{\partial(rv)}{\partial r} &= \frac{\nu}{UL}\left[\nabla^2(rv) - \frac{2}{r}\frac{\partial(rv)}{\partial r}\right] \\
u\frac{\partial u}{\partial x} + w\frac{\partial u}{\partial r} &= -\frac{\partial P}{\partial x} + \frac{\nu}{UL}\nabla^2 u \\
u\frac{\partial w}{\partial x} + w\frac{\partial w}{\partial r} - \frac{v^2}{r} &= -\frac{\partial P}{\partial r} - \frac{\nu}{UL}\left(\nabla^2 w - \frac{w}{r^2}\right) \\
\frac{\partial u}{\partial x} + \frac{\partial w}{\partial r} + \frac{w}{r} &= 0
\end{aligned}
$$

- USE FINITE DIFFERENCE METHOD (PARABOLIC EQUATION)
  CENTRAL DIFFERENCE ALONG r DIRECTION
  BACKWARD DIFFERENCE ALONG x DIRECTION

INITIAL CONDITION

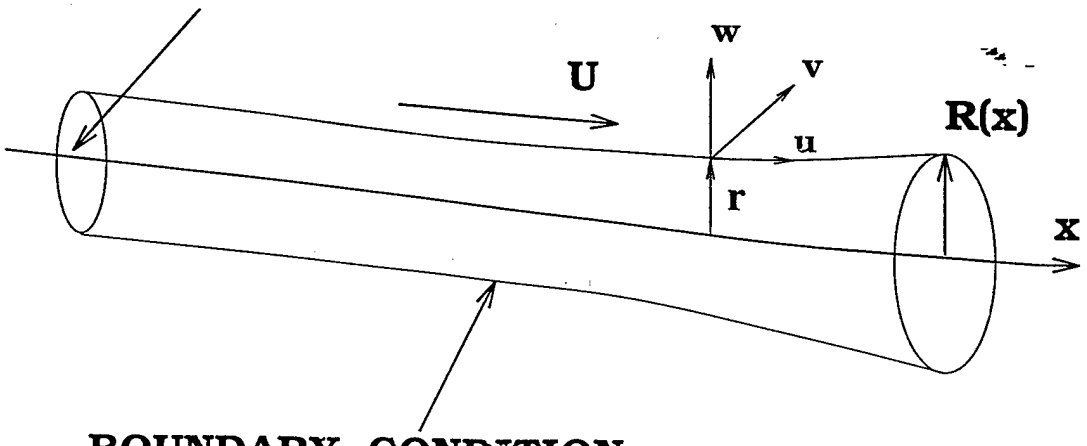

BOUNDARY CONDITION

P (x , r) : PRESSURE OUTSIDE CORE (INVISCID FLOW)
L : CORE DIAMETER

2. EXAMPLE (A TRAILING VORTEX)

- CONSTANT CORE RADIUS ALONG THE CORE CENTER LINE.
- CONSTANT PRESSURE OUTSIDE THE CORE.
- INITIAL CONDITION :

$$x_o = 0.25, \quad R(x_o) = 6$$
$$u_o = 1 - 0.25e^{-r^2}, \quad v_o = (0.5 - 0.5e^{-r^2})/r$$

- AT $x = x_o$: CORE RADIUS (R_0)
  VELOCITIES INSIDE THE CORE (u_o , v_o)
  PRESSURE OUTSIDE THE CORE (P (x))

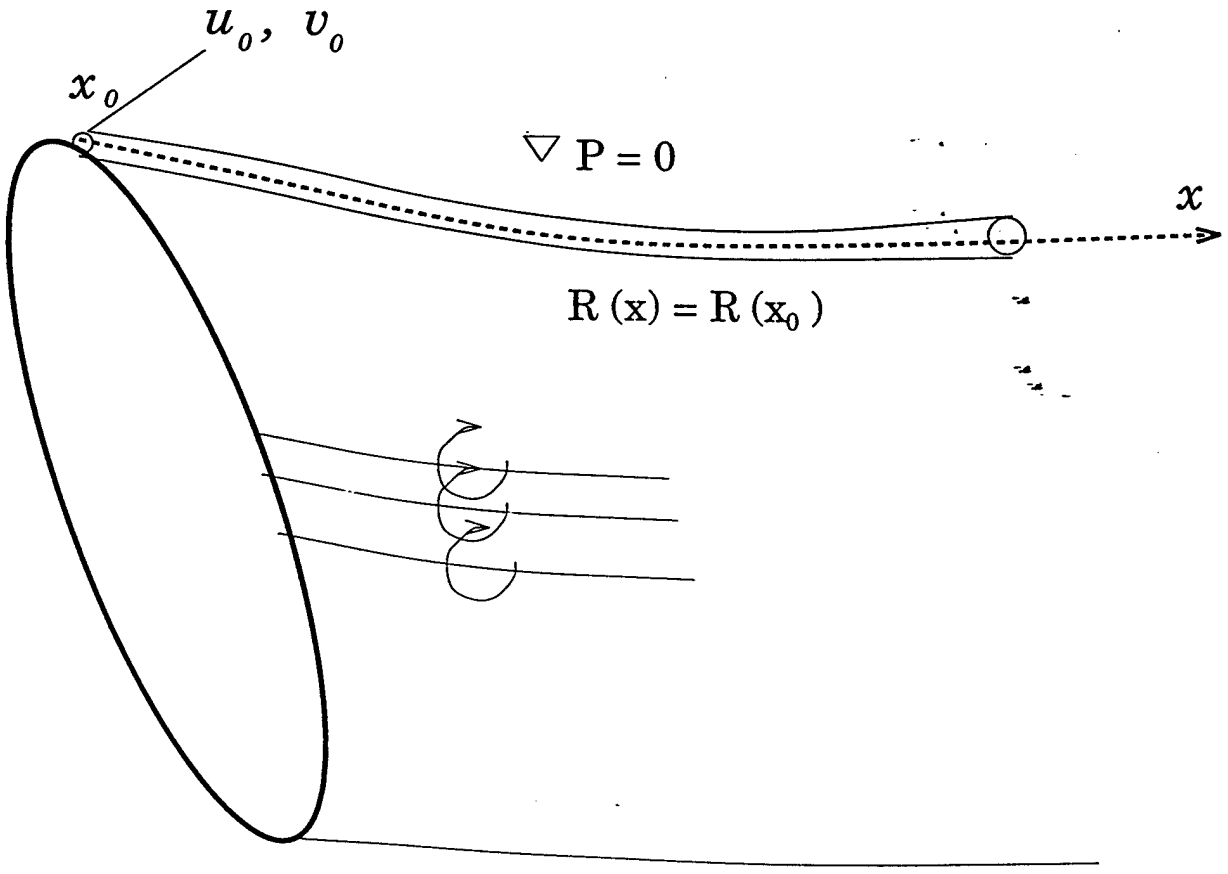

CIRCUMFERENTIAL VELOCITY IN A TRAILING VORTEX

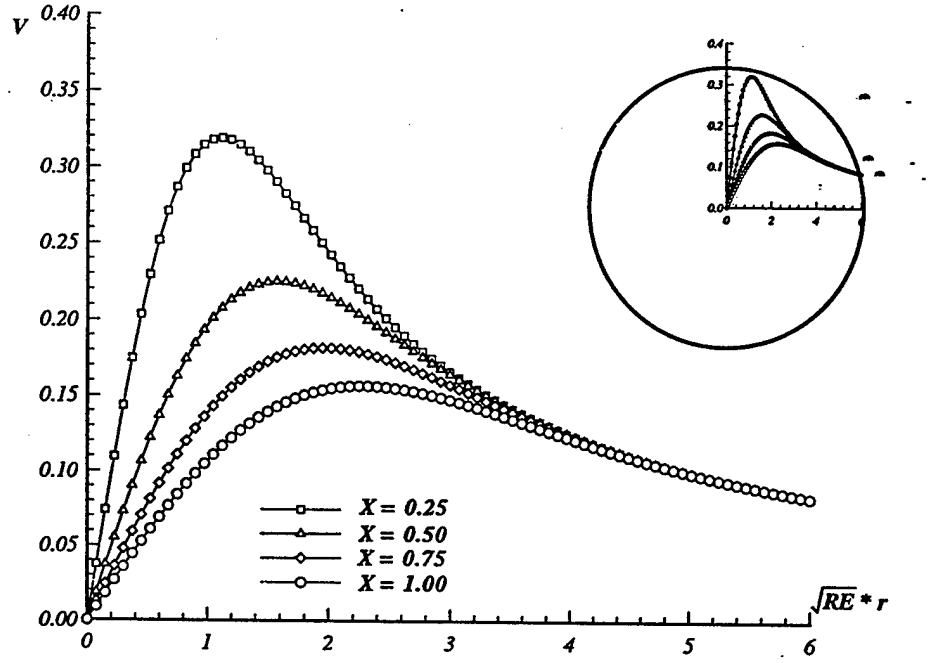

AXIAL VELOCITY IN A TRAILING VORTEX

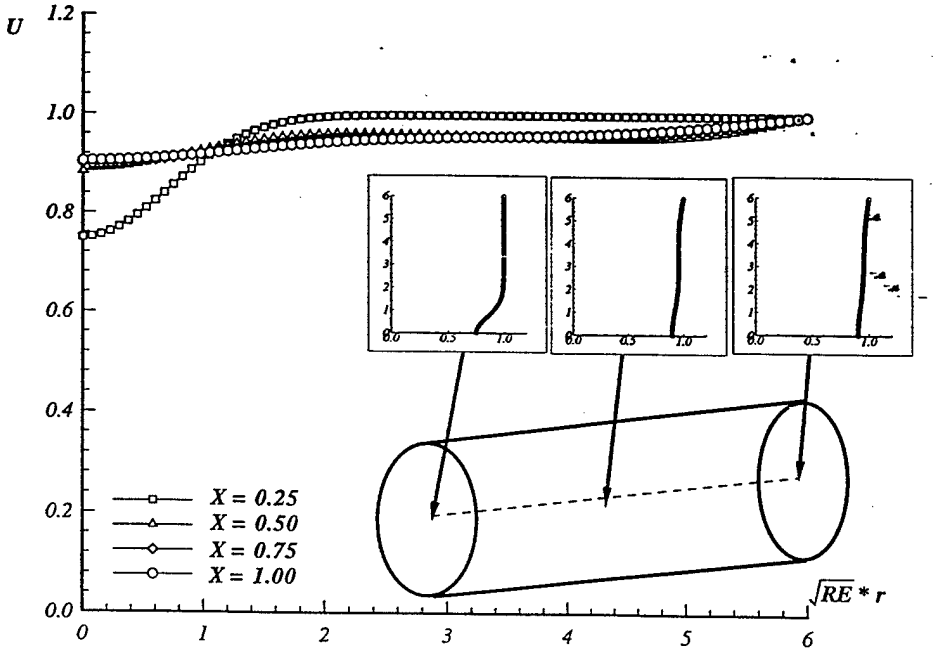

D Propeller geometries

Number of Blades : 5
Hub/Diameter Ratio : 0.3
Section Meanline : NACA a=0.8
Section Thickness Form : NACA66 (Modified)
Design J_S : 1.038

r/R	P/D	x_m/D	$skew^o$	c/D	f/c	t/D
0.30	1.165	0.0091	2.985	0.178	0.0000	0.0420
0.35	1.296	0.0103	3.481	0.210	0.0050	0.0372
0.45	1.480	0.0103	4.810	0.271	0.0209	0.0290
0.55	1.566	0.0103	6.631	0.327	0.0267	0.0226
0.65	1.566	0.0103	8.978	0.374	0.0256	0.0178
0.75	1.498	0.0103	11.895	0.406	0.0209	0.0146
0.85	1.381	0.0103	15.410	0.409	0.0151	0.0122
0.90	1.306	0.0102	17.403	0.387	0.0122	0.0110
0.95	1.222	0.0103	19.557	0.326	0.0094	0.0091
1.00	1.128	0.0102	21.876	0.000	0.0000	0.0000

Table 2: The geometry of the propeller DTMB 4661.

Number of Blades : 5
Hub/Diameter Ratio : 0.3
Section Meanline : NACA a=0.8
Section Thickness Form : NACA66 (Modified)
Design J_S : 1.0
Cavitation Number : 2.0
Froude Number : 8.86

r/R	P/D	x_m/D	$skew^o$	c/D	f/c	t/D
0.30	1.087	0.0111	6.280	0.200	-0.0380	0.0539
0.35	1.245	-0.0069	-0.754	0.237	-0.0086	0.0422
0.40	1.365	-0.0237	-4.824	0.276	0.0090	0.0315
0.45	1.458	-0.0358	-7.336	0.308	0.0178	0.0274
0.50	1.541	-0.0437	-8.865	0.334	0.0279	0.0252
0.60	1.673	-0.0483	-9.838	0.385	0.0366	0.0226
0.70	1.633	-0.0419	-8.108	0.435	0.0332	0.0021
0.80	1.502	-0.0302	-3.784	0.475	0.0247	0.0019
0.85	1.428	-0.0234	-0.493	0.482	0.0186	0.0186
0.90	1.335	-0.0165	3.784	0.465	0.0119	0.0203
0.93	1.259	-0.0123	6.922	0.431	0.0079	0.0227
0.95	1.189	-0.0096	9.297	0.390	0.0054	0.0229
0.97	1.097	-0.0068	11.927	0.325	0.0030	0.0205
0.99	0.974	-0.0039	14.834	0.206	0.0009	0.0131
1.00	0.900	-0.0025	16.400	0.000	0.0000	0.0000

Table 3: The geometry of the propeller DTMB 5168.